AMPK Activation Regulates LTBP4-Dependent TGF-β1 Secretion by Pro-inflammatory Macrophages and Controls Fibrosis in Duchenne Muscular Dystrophy

Gaëtan Juban, Marielle Saclier, Houda Yacoub-Youssef, Amel Kernou, Ludovic Arnold, Camille Boisson, Sabrina Ben Larbi, Mélanie Magnan, Sylvain Cuvellier, Marine Théret, et al.

Article

Cell Reports

AMPK Activation Regulates LTBP4-Dependent TGF-β1 Secretion by Pro-inflammatory Macrophages and Controls Fibrosis in Duchenne Muscular Dystrophy

Graphical Abstract

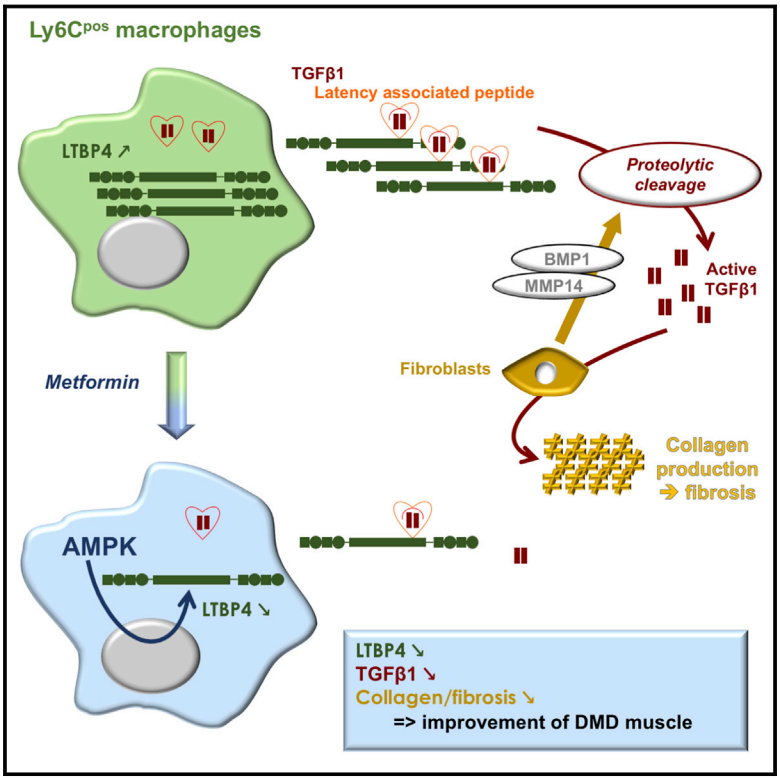

Authors

Gaëtan Juban, Marielle Saclier, Houda Yacoub-Youssef, ..., Julien Gondin, Rémi Mounier, Bénédicte Chazaud

Correspondence

benedicte.chazaud@inserm.fr

In Brief

Juban et al. show that, in DMD muscle, macrophages produce LTBP4, inducing the secretion of latent TGF-β1. Fibroblast-derived enzymes activate TGF-β1, which promotes collagen secretion by fibroblasts. AMPK activation inhibits LTBP4 expression and TGF-β1 production by macrophages. Metformin treatment of DMD mice reduces fibrosis and increases muscle regeneration and strength.

Highlights

- In DMD muscle, Ly6C^{pos} macrophages produce latent TGF-β1 due to high LTBP4 synthesis
- AMPK activation downregulates LTBP4 expression and TGF-β1 production by macrophages
- Metformin treatment of DMD mice decreases fibrosis and improves muscle function
- Fibroblast-derived enzymes activate latent TGF-β1, which acts on fibroblasts

Juban et al., 2018, Cell Reports *25*, 2163–2176
November 20, 2018
https://doi.org/10.1016/j.celrep.2018.10.077

CellPress

Cell Reports
Article

AMPK Activation Regulates LTBP4-Dependent TGF-β1 Secretion by Pro-inflammatory Macrophages and Controls Fibrosis in Duchenne Muscular Dystrophy

Gaëtan Juban,[1,6] Marielle Saclier,[2,6] Houda Yacoub-Youssef,[2] Amel Kernou,[2] Ludovic Arnold,[3] Camille Boisson,[1] Sabrina Ben Larbi,[1] Mélanie Magnan,[2] Sylvain Cuvellier,[2] Marine Théret,[1] Basil J. Petrof,[4,5] Isabelle Desguerre,[2] Julien Gondin,[1] Rémi Mounier,[1] and Bénédicte Chazaud[1,7,*]

[1]Institut NeuroMyoGène, Université Claude Bernard Lyon 1, CNRS UMR 5310, INSERM U1217, Université Lyon, Villeurbanne 69100, France
[2]Institut Cochin, INSERM U1016, CNRS UMR 8104, Université Paris Descartes, Sorbonne Paris Cité, Paris 75014, France
[3]Centre d'Immunologie et des Maladies Infectieuses, INSERM U1135, Université Pierre et Marie Curie, Sorbonne Universités, Paris 75013, France
[4]Meakins-Christie Laboratories, McGill University, Montreal, QC H4A3J1, Canada
[5]Research Institute of the McGill University Health Centre, Montreal, QC H4A3J1, Canada
[6]These authors contributed equally
[7]Lead Contact
*Correspondence: benedicte.chazaud@inserm.fr
https://doi.org/10.1016/j.celrep.2018.10.077

SUMMARY

Chronic inflammation and fibrosis characterize Duchenne muscular dystrophy (DMD). We show that pro-inflammatory macrophages are associated with fibrosis in mouse and human DMD muscle. DMD-derived Ly6C^{pos} macrophages exhibit a profibrotic activity by sustaining fibroblast production of collagen I. This is mediated by the high production of latent-TGF-β1 due to the higher expression of LTBP4, for which polymorphisms are associated with the progression of fibrosis in DMD patients. Skewing macrophage phenotype via AMPK activation decreases ltbp4 expression by Ly6C^{pos} macrophages, blunts the production of latent-TGF-β1, and eventually reduces fibrosis and improves DMD muscle force. Moreover, fibro-adipogenic progenitors are the main providers of TGF-β-activating enzymes in mouse and human DMD, leading to collagen production by fibroblasts. *In vivo* pharmacological inhibition of TGF-β-activating enzymes improves the dystrophic phenotype. Thus, an AMPK-LTBP4 axis in inflammatory macrophages controls the production of TGF-β1, which is further activated by and acts on fibroblastic cells, leading to fibrosis in DMD.

INTRODUCTION

Inflammation following tissue damage is essential for the recovery of tissue integrity. Macrophages play pleiotropic roles in both the inflammatory response and the process of tissue repair that ensues. These various functions are supported by the different phenotypes and inflammatory status that macrophages adopt, depending on their environment (Wynn and Vannella, 2016). In many organs, a general picture of macrophage activation was established during tissue repair after acute injury. Soon after damage, the tissue is invaded by Ly6C^{pos} pro-inflammatory macrophages that support the mounting of the inflammatory response. Once phagocytosis of tissue and cell debris is achieved, a second phase of tissue repair occurs, which is characterized by the presence of Ly6C^{neg} macrophages, exhibiting anti-inflammatory properties and restorative functions (Chazaud, 2014). The precise phenotype of these anti-inflammatory macrophages is not well characterized *in vivo* and likely depends on the tissue and type of injury. For instance, restorative macrophages may depend (in skin) or not (in skeletal muscle) on interleukin-4 [IL-4] signaling to express the anti-inflammatory phenotype (Knipper et al., 2015; Varga et al., 2016a). However, all restorative macrophages exhibit a low expression of pro-inflammatory effectors and express anti-inflammatory mediators (IL-10, transforming growth factor β [TGF-β]). Moreover, in all of the tissues examined so far, Ly6C^{neg} macrophages that support tissue repair arise from resident macrophages and/or circulating Ly6C^{pos} monocytes that have entered into the tissue and then are converted into Ly6C^{neg} macrophages at the time of resolution of inflammation (Wynn and Vannella, 2016).

In comparison to the acute injury response, the phenotypes and roles played by macrophages during chronic diseases are poorly understood. The persistence of tissue injury, whatever its origin (e.g., toxic, genetic), leads to chronic inflammation and, most of the time, to the establishment of fibrosis that progressively replaces the parenchyma. Roles of macrophage subsets in this context are still debated and likely depend on the tissue and the disease. For instance, alternatively activated macrophages were shown to promote fibrosis in chronic pancreatitis (Xue et al., 2015), while similar IL-4/IL-4R (IL-4 receptor)-activated macrophages reduce fibrosis after helminth infection in lung and liver (Minutti et al., 2017). In several organs, fibrosis is induced or aggravated by blood-derived Ly6C^{pos} macrophages (Misharin et al., 2017; Tacke and Zimmermann, 2014).

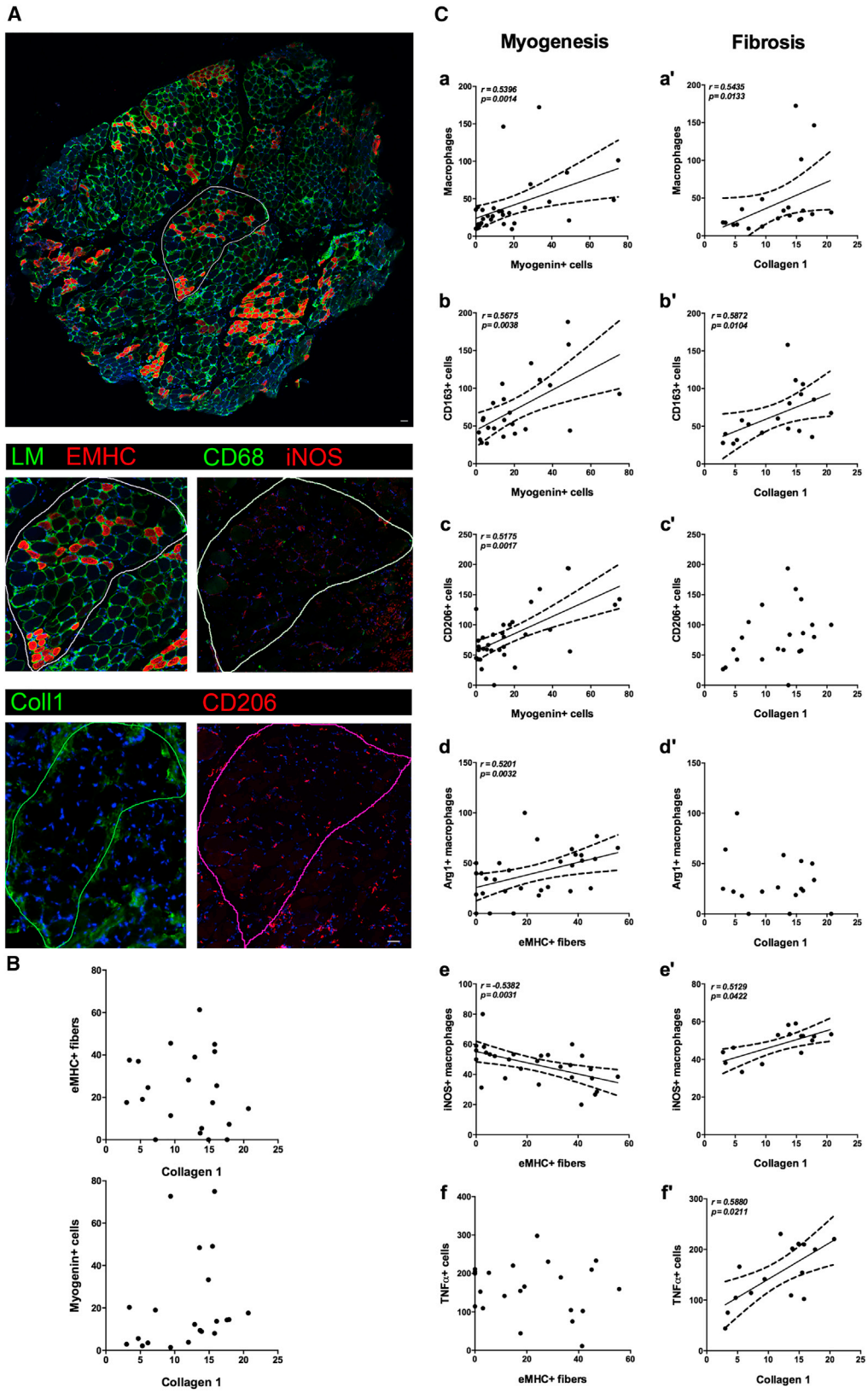

(legend on next page)

Macrophages have been known for decades to express TGF-β, which is secreted as a latent protein and must be activated to signal in target cells, for example, to induce collagen production by fibroblasts (Biernacka et al., 2011). However, the mechanisms by which macrophages regulate TGF-β secretion have been overlooked.

Adult skeletal muscle fully regenerates without scarring after acute injury. During this process, macrophages adopt sequential pro- then anti-inflammatory phenotypes to exert specific functions toward myogenic precursor cells and to support adult myogenesis (Arnold et al., 2007; Mounier et al., 2013; Saclier et al., 2013; Varga et al., 2016b), and toward fibroblastic cells to prevent excessive matrix deposition (Lemos et al., 2015). Inversely, in degenerative myopathies, skeletal muscle fails to regenerate due to permanent and asynchronous cycles of degeneration-regeneration, such as with mutations of genes encoding for proteins of the dystrophin-glycoprotein complex, which ensures myofiber integrity (Lapidos et al., 2004). In these disorders, recurrent myofiber damage leads to chronic inflammation and the eventual establishment of fibrosis. Macrophages are associated with fibrosis in mdx muscle, the mouse model for Duchenne muscular dystrophy (DMD) (Vidal et al., 2008). Preventing the entry of circulating monocytes into mdx muscle improves muscle histology and function for several weeks (Mojumdar et al., 2014; Wehling et al., 2001). Inhibition of the pro-inflammatory nuclear factor κB (NF-κB) pathway is similarly associated with a lower macrophage number and a better phenotype of the muscle (Acharyya et al., 2007). However, although the presence of several macrophage subsets in dystrophic muscle was proposed (Vidal et al., 2008; Villalta et al., 2009, 2011), their precise functions in the establishment of fibrosis remain uncharacterized.

Here, we show evidence in dystrophic fibrotic muscle of a specific cellular interplay between Ly6C^{pos} macrophages and fibroblastic cells in which Ly6C^{pos} macrophages promoted survival and matrix deposition by fibroblastic cells through the secretion of TGF-β1. Specifically, Ly6C^{pos} macrophages secreted high amounts of latent TGF-β1 due to increased expression of latent-TGF-β-binding protein (LTBP)4, which is a known gene modifier in DMD patients (Flanigan et al., 2013). Fibroblastic cells known as fibro-adipogenic progenitors (FAPs) secreted increased amounts of enzymes responsible for latent TGF-β activation. Moreover, the expression of LTBP4 in Ly6C^{pos} macrophages was controlled by AMP kinase (AMPK) activation in mdx muscle. Cross-talk between inflammatory Ly6C^{pos} macrophages and FAPs leads to increased collagen deposition in dystrophic muscles that can be pharmacologically controlled by the regulation of AMPK activity.

RESULTS

Macrophages Are the Main Immune Cells Present in Mouse Degenerative Myopathies and Are Associated with Fibrosis

Investigation of macrophages was carried out in two murine models (the dystrophin-deficient mdx and the α-sarcoglycan-deficient sgca$^{-/-}$ mouse strains) of degenerative myopathies that develop fibrosis with different kinetics. Mdx mice were used at 8–10 weeks of age—at a stage of chronic disease—and *tibialis anterior* muscle was experimentally microinjured over 2 weeks to induce the establishment of fibrosis after 1 week of rest (fib-mdx) (Desguerre et al., 2012). As shown in Figure S1A, fib-mdx muscle presented higher irregularity in myofiber shape and size, as compared with mdx muscle, and was characterized by inflammatory infiltrates and endomysial fibrosis. sgca$^{-/-}$ mice develop spontaneous fibrosis at 3 months (Duclos et al., 1998). At 4 months of age, *tibialis anterior* muscles of sgca$^{-/-}$ mice exhibited necrosis, inflammatory infiltrates, and myofibers of various sizes with centrally located nuclei, which reflects recent muscle regeneration and endomysial fibrosis (Figure S1A'). Flow cytometry analysis (Figures S1B and S1B') of immune cells showed that in both models, the main cell type present in dystrophic fibrotic muscle was macrophages, which were increased in number (Figures S1C and S1C') and represented 73% and 68% of CD45^{pos} cells in fib-mdx and sgca$^{-/-}$ muscles, respectively. Among these cells, the Ly6C^{neg} subset was the most abundant, accounting for approximately 73%–77% of all muscle macrophages.

Comparing mdx, fib-mdx, sgca$^{+/-}$ and sgca$^{-/-}$ muscles, we showed that collagen I deposition positively correlated with the number of fibroblastic cells (platelet-derived growth factor receptor α-positive [PDGFRα^{pos}] cells [Joe et al., 2010; Uezumi et al., 2010]) (Spearman's $\rho = 0.796$, $p < 0.0001$) (Figure S2A), following an sgca$^{+/-}$ < mdx < sgca$^{-/-}$ = fib-mdx gradient of fibrosis, which was also associated with the total number of infiltrating F4/80^{pos} macrophages in the muscle (Figure S2B). Myopathic muscles being characterized by a highly heterogeneous histological pattern (Rosenberg et al., 2015), we looked at the distribution of macrophages. Within fib-mdx muscle, macrophages were not preferentially associated with small or large myofibers (Figures S2C and S2D); however, the number of macrophages positively correlated with the collagen I area (Figures S2E and S2F). These results indicate that (1) macrophages were the main immune cells in dystrophic fibrotic muscle; (2) the more the muscle was fibrotic, the more macrophages were numerous; and (3) macrophages specifically associated with fibrotic areas.

Figure 1. Macrophages, Fibrosis, and Myogenesis in Human DMD Muscle

(A–C) Serial sections of DMD muscles were immunolabeled for macrophages (CD68), collagen I, myogenesis markers (eMHC, myogenin), or macrophage markers (e.g., CD163, CD206, Arg1, iNOS, TNF-α). Scale bars, 50 μm. Correlation analyses were done in individual fascicles (line depicted in A, where LM is laminin and Hoechst is blue).

(B) Spearman correlation was made between fibrosis (collagen I area, in percentage of total area) and myogenesis (number of eMHC^{pos} fibers or myogenin^{pos} cells).

(C) Spearman correlation was made between myogenesis (number of myogenin^{pos} cells or eMHC^{pos} fibers, left) or fibrosis (collagen I area, right) and the number of (a, a') total macrophages (CD68^{pos} cells), (b, b') CD163^{pos}CD68^{pos} macrophages, (c, c') CD206^{pos}CD68^{pos} macrophages, (d, d') Arg1^{pos}CD68^{pos} macrophages, (e, e') iNOS^{pos}CD68^{pos} macrophages, and (f, f') TNFα^{pos}CD68^{pos} macrophages. Results are from 34 fascicles from 6 DMD patients.

See also Figures S1 and S2.

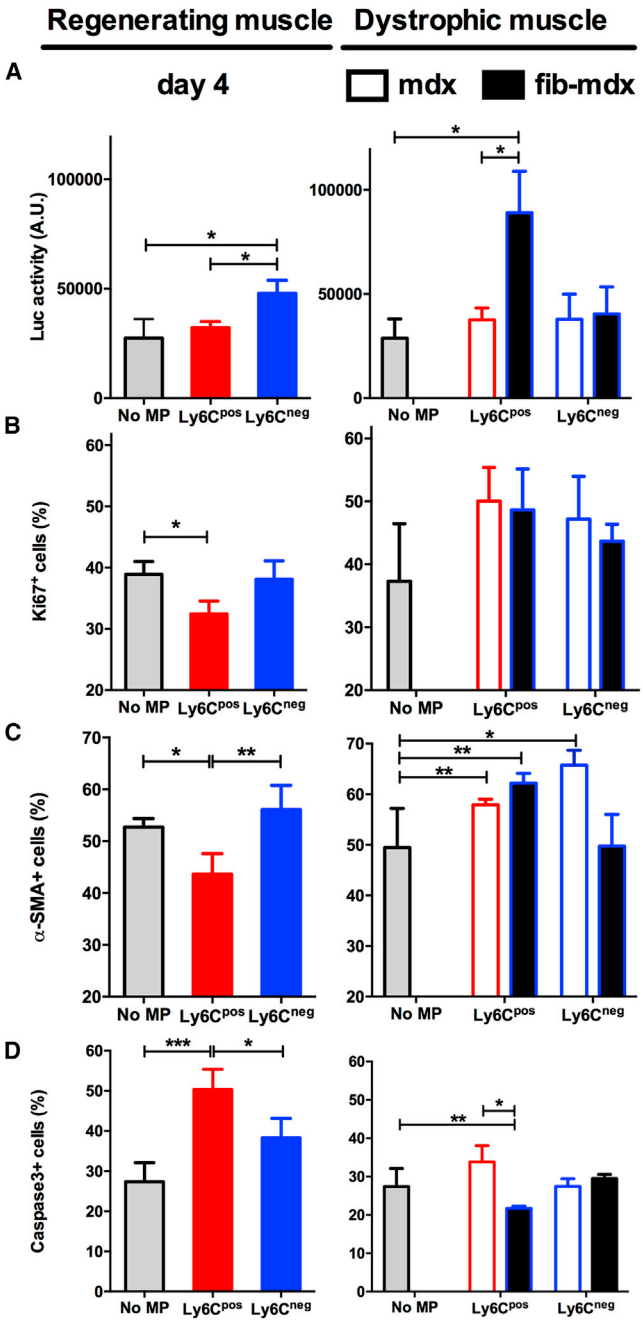

Figure 2. Functions of Macrophage Subsets Isolated from Regenerating and Dystrophic Muscle toward Fibroblasts

Ly6C^{pos} and Ly6C^{neg} macrophage subsets were sorted from regenerating (left) and dystrophic (mdx or fib-mdx, right) muscle and were co-cultured with NIH 3T3 fibroblasts.

(A) Luciferase activity as a surrogate of collagen I expression from fibroblasts previously transfected with a plasmid encoding luciferase under collagen I promoter.

(B) Fibroblast proliferation (Ki67^{pos} cells).

(C) Fibroblast differentiation into myofibroblasts (α-SMA^{pos} cells).

(D) Fibroblast apoptosis (caspase 3^{pos} cells).

Results are means ± SEMs of three (regenerating muscle, left) or four (dystrophic muscle, right) experiments. *$p < 0.05$, **$p < 0.01$, ***$p < 0.001$ using Student's t test. See also Figure S3.

Macrophages Expressing Pro-inflammatory Markers Are Associated with Fibrosis in Human DMD and Mouse Dystrophic Models

Serial sections of human DMD muscles were stained by immunofluorescence for a series of myogenic (embryonic myosin [eMHC], myogenin), fibrosis (collagen I), and macrophage markers (CD68 coupled to pro-inflammatory markers such as inducible nitric oxide synthase [iNOS], tumor necrosis factor α [TNF-α], or anti-inflammatory markers such as Arg1, CD163, and CD206), as was previously done for regenerating muscle (Saclier et al., 2013). Because DMD muscles are highly heterogeneous, correlation analyses were done in individual fascicles (example in Figure 1A). Myogenesis did not correlate with fibrosis (Figure 1B). The total number of macrophages correlated with both the number of myogenin^{pos} cells (Figure 1C, a) and collagen I area (Figure 1C, a'), indicating that macrophages were associated with both myogenesis and fibrosis. As already shown in normal human muscle regeneration (Saclier et al., 2013), myogenesis markers (myogenin, eMHC) positively correlated with anti-inflammatory marker-expressing macrophages (e.g., CD163, CD206, Arg1; Figure 1C, b–d), while they were not associated with pro-inflammatory marker-expressing macrophages (e.g., iNOS, TNF-α; Figure 1C, e and f). In contrast, collagen I area positively correlated with only one anti-inflammatory marker (CD163) (Figure 1C, b'–d'). Moreover, a positive correlation was observed between the collagen I area and the pro-inflammatory iNOS expressing macrophages (Figure 1C, e') and TNF-α expressing cells (Figure 1C, f').

These results were confirmed in both fib-mdx and sgca$^{-/-}$ muscles. Because only a few markers of macrophage activation have been developed for cytometry analysis, immunolabeling on muscle sections was performed for 10 different markers. The number of F4/80^{pos} macrophages expressing anti-inflammatory (IL-10, CD206, Dectin 1, CD301, and Arg1) and pro-inflammatory (TNF-α, C-C chemokine receptor type 2CCR2, Cox2, CCL3, and iNOS) markers both increased in dystrophic muscle (sgca$^{-/-}$, mdx, fib-mdx) as compared with normal muscle (sgca$^{+/-}$) (Figures S2G, S2H, and S2I). However, when comparing fibrotic (sgca$^{-/-}$, fib-mdx) to non-fibrotic dystrophic muscle (mdx), only the number of macrophages expressing pro-inflammatory markers was increased (with the exception of Arg1 and C-C chemokine ligand 3 [CCL3]) (Figures S2G, S2H, and S2I). These results show that in both human and mouse dystrophic muscle, fibrosis was associated with pro-inflammatory macrophages.

Ly6C^{pos} Macrophages Exert Profibrotic Functions toward Fibroblasts in DMD Muscle

While pro-inflammatory macrophages were associated with fibrosis in these muscles, Ly6C^{neg} macrophages were more numerous than Ly6C^{pos} macrophages in fibrotic dystrophic muscle (cf. Figures S1C and S1C'). In post-injury regenerating muscle, Ly6C^{pos} macrophages are pro-inflammatory cells at early steps of regeneration, while Ly6C^{neg} macrophages exhibit an anti-inflammatory profile during the later recovery steps of muscle regeneration (Varga et al., 2016a). qRT-PCR analysis of the expression of seven genes associated with macrophage activation inflammatory status indicated that both subsets

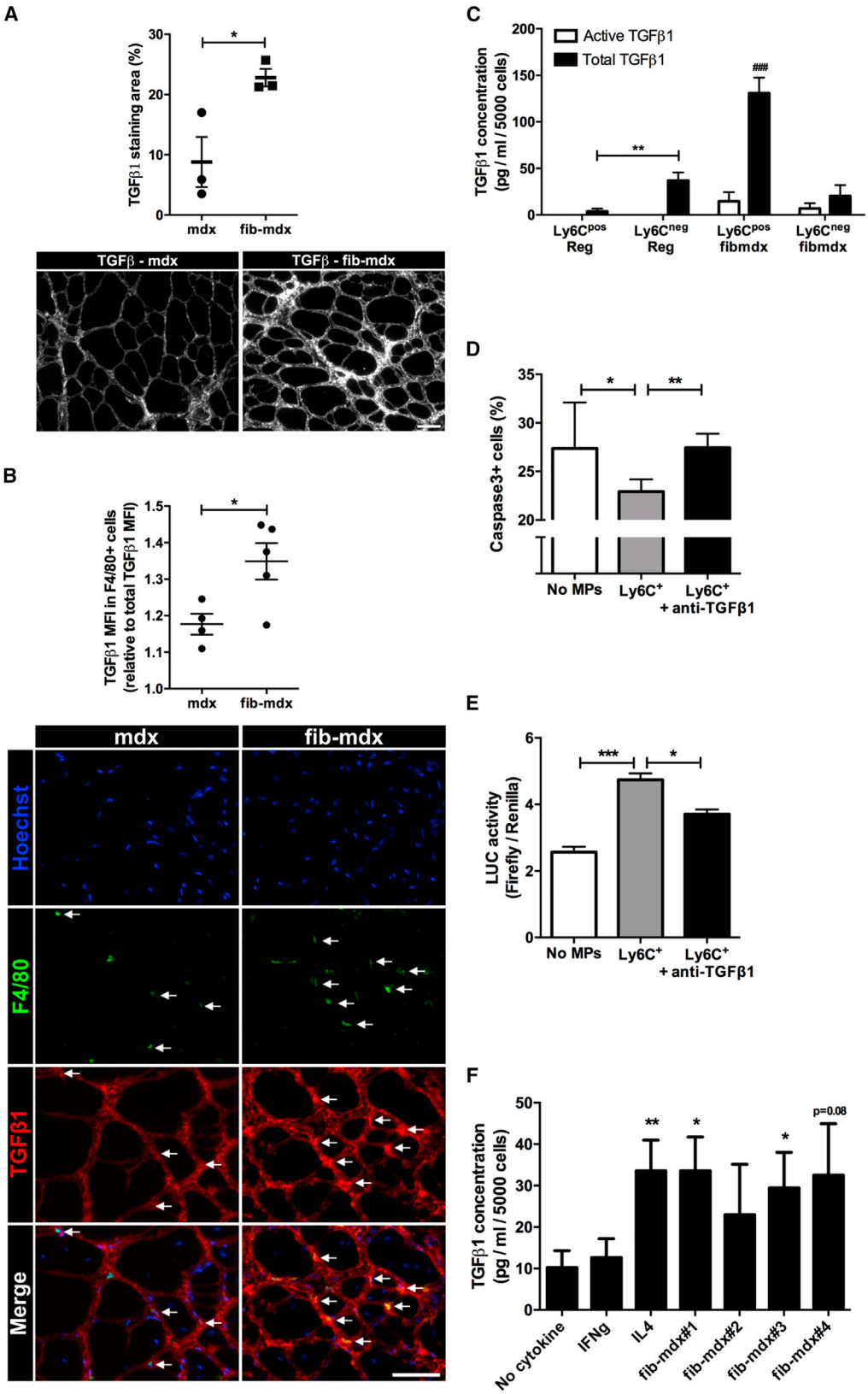

(legend on next page)

expressed both pro- and anti-inflammatory markers (Figures S3A and S3B). This indicates the presence of a mixed phenotype, as previously suggested, because 43% of macrophages in fib-mdx co-express *tnfa* and *tgfb1* (Lemos et al., 2015).

We therefore focused on the function of macrophage subsets in fib-mdx muscle. Because fibroblastic cells are the main provider of collagen in mdx muscle (Pessina et al., 2015) and because macrophages regulate fibroblastic cell death during muscle regeneration (Lemos et al., 2015), the effects of Ly6C^{pos} and Ly6C^{neg} macrophage subsets on fibroblasts were compared in regenerating and dystrophic fibrotic muscle. Fluorescence-activated cell sorting (FACS)-sorted FAPs from mdx and fib-mdx muscle poorly survive and poorly grow in short-term (2 days) culture, although surviving cells expand after 4–5 days of culture. However, properties of macrophages must be tested shortly after their sorting (i.e., 24 hr) because they rapidly adapt or alter their inflammatory phenotype to their novel environment. Therefore, long-term FAP culture is not compatible with short-term macrophage analysis. Consequently, we used fibroblastic cells (NIH 3T3) as a surrogate of FAPs. In regenerating muscle, only the Ly6C^{neg} macrophage subset stimulated the expression of a collagen I reporter gene transfected into fibroblasts (+200% at D2 and +60% at D4 post-injury) (Figures S3C and 2A), in accordance with previous results obtained with FAPs (Lemos et al., 2015). Conversely, in both sgca$^{-/-}$ and fib-mdx muscles, only Ly6C^{pos} macrophages increased collagen production by fibroblasts by 208% and 309%, respectively (Figures S3C and 2A). Furthermore, proliferation and differentiation of fibroblasts was decreased by Ly6C^{pos} macrophages that issued from regenerating muscle (Figures 2B and 2C), while inversely, Ly6C^{pos} isolated from fib-mdx muscle stimulated the differentiation of fibroblasts into α-smooth muscle actin-positive (α-SMA^{pos}) cells (Figure 2C). It is worth mentioning that in mdx, both subsets increased the number of α-SMA^{pos} fibroblasts (Figure 2C). Finally, we showed that Ly6C^{pos} macrophages from regenerating muscle induced fibroblast apoptosis, as it was shown for FAPs (Lemos et al., 2015), and that Ly6C^{pos} macrophages issued from fib-mdx lost this property and even protected fibroblasts from death (Figure 2D). These results show that in fibrotic dystrophic muscle, Ly6C^{pos} macrophages favored fibroblast persistence and their production of collagen I, thus contributing to the establishment of fibrosis.

TGF-β1 Controls the Profibrogenic Properties of Ly6C^{pos} Macrophages in Dystrophic Skeletal Muscle

As in various other tissues, TGF-β1 has been involved in the establishment of fibrosis in skeletal muscle, particularly in DMD (Andreetta et al., 2006; Chen et al., 2005; Vetrone et al., 2009; Vidal et al., 2008). TGF-β1 is secreted in the milieu as a single latent molecule comprising an N-terminal latency-associated peptide and the C-terminal mature TGF-β, which dimerizes and complexes with latent TGF-β binding protein (LTBP) to be secreted and to interact with the extracellular matrix (Travis and Sheppard, 2014). Figure 3A shows that TGF-β1 protein level (as the staining area on the muscle tissue section) was increased 2.6-fold in fib-mdx as compared with mdx muscle. Measurement of *tgfb1* mRNA showed no difference between Ly6C^{pos} and Ly6C^{neg} macrophages that issued from regenerating, mdx, or fib-mdx muscle (Figure S3B). However, macrophages expressed TGF-β1 in dystrophic muscle as assessed by F4/80 and TGF-β1 co-staining (Figure 3B). Moreover, TGF-β1 mean fluorescence intensity (MFI) of macrophages was increased by 15% in fib-mdx as compared with mdx muscle (Figure 3B). More precisely, ELISA measurement of TGF-β1 secreted by sorted macrophages showed that Ly6C^{neg} macrophages from regenerating muscle produced 10-fold more TGF-β1 than their Ly6C^{pos} counterpart (Figure 3C). Conversely, Ly6C^{pos} macrophages isolated from fib-mdx muscle secreted 6.3-fold more TGF-β1 than Ly6C^{neg} macrophages in fib-mdx (Figure 3C) (and 3.5- and 34-fold more than Ly6C^{neg} and Ly6C^{pos} macrophages from regenerating muscle), in accordance with their stimulating effect on fibroblasts (see Figure 2). In both conditions, TGF-β1 was mainly secreted in a latent form (Figure 3C). In co-culture experiments of macrophages isolated from fib-mdx with fibroblasts, blocking anti-TGF-β1 antibodies abolished the protective effect of Ly6C^{pos} macrophages on fibroblast apoptosis (Figure 3D) and blunted the stimulation of collagen I expression by Ly6C^{pos} macrophages (Figure 3E). Finally, to investigate whether the dystrophic environment affects naive unactivated macrophages, bone marrow-derived macrophages (BMDMs) were treated with protein homogenate from fib-mdx muscle or with IL-4, which is a well-known inducer of TGF-β1 production in macrophages. Fib-mdx muscle homogenate triggered TGF-β1 secretion as efficiently as IL-4 did (Figure 3F). These results indicate that the fib-mdx muscle environment stimulated Ly6C^{pos} macrophages to secrete high amounts of latent TGF-β1, which directly acted on fibroblastic cells to promote fibrosis.

LTBP4 Controls Latent TGF-β1 Secretion by Ly6C^{pos} Macrophages in fib-mdx

Latent TGF-β is secreted when complexed to LTBP (Travis and Sheppard, 2014). Among the murine LTBPs, LTBP4 was expressed by macrophages in skeletal muscle, with an increased expression by Ly6C^{pos} macrophages in fibrotic dystrophic

Figure 3. Latent TGF-β1 Is Secreted by Profibrotic Ly6C^{pos} Macrophages in fib-mdx

(A) Area of TGF-β1 immunolabeling on mdx or fib-mdx muscle sections.

(B) Mean fluorescence intensity (MFI) of TGF-β1 immunolabeling in F4/80^{pos} cells relative to TGF-β1 MFI in the whole picture on mdx or fib-mdx muscle sections.

(C) TGF-β1 production of macrophage subsets sorted from regenerating (day 1 after injury for Ly6C^{pos} cells; day 4 for Ly6C^{neg} cells) or from fib-mdx muscles after 24 hr of culture.

(D and E) Macrophage subsets sorted from fib-mdx muscle were co-cultured with fibroblasts, as in Figure 2, with or without TGF-β1-blocking antibodies.

(D) The number of apoptotic fibroblasts was assessed after caspase 3 immunolabeling.

(E) Luciferase activity was measured as a reporter for collagen I expression, as in Figure 2A.

(F) TGF-β1 production of BMDMs stimulated for 3 days with various cytokines or with total protein extracts from fib-mdx muscle.

Results are means ± SEMs of three (A and E), four (B and F), six (C), and five (D) experiments. The Student's t test was performed between the conditions indicated by the bars or versus no cytokine in (F). *p < 0.05, **p < 0.01, ***p < 0.001; versus all other conditions in C, ###p < 0.001. Scale bar, 50 μm.

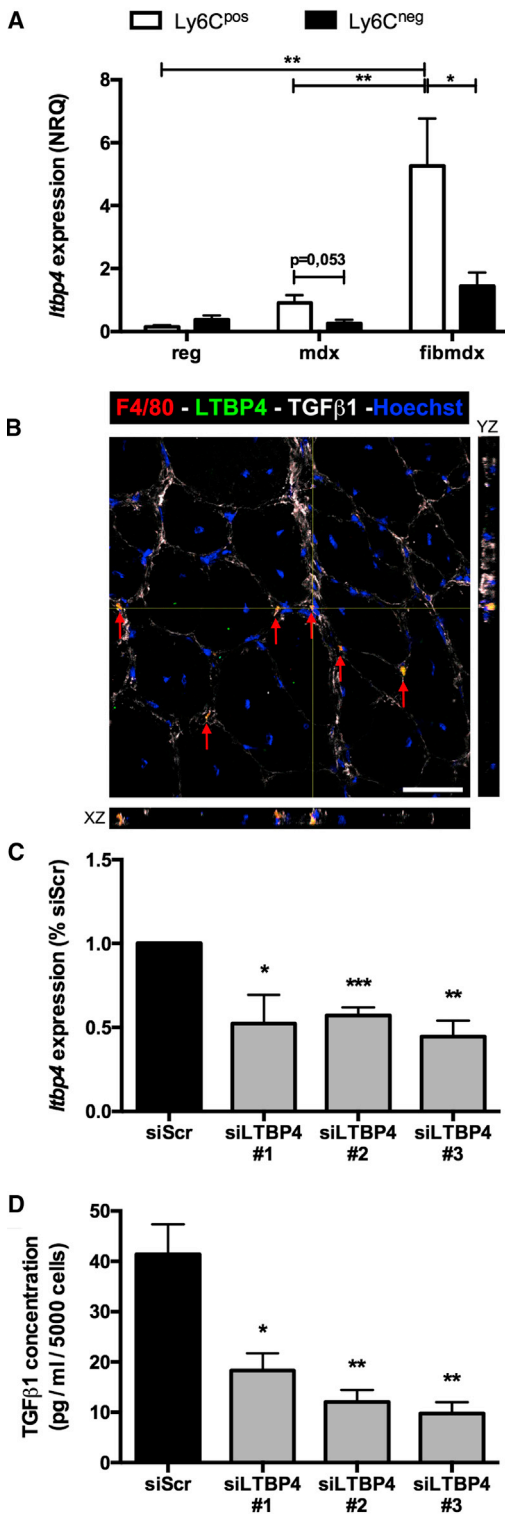

Figure 4. Latent TGF-β1 Secretion by Ly6C^{pos} Macrophages Is Regulated by LTBP4

(A) Macrophage subsets were sorted from regenerating (day 1 after injury for Ly6C^{pos} cells; day 4 for Ly6C^{neg} cells) mdx or fib-mdx muscles, and the *ltbp4* mRNA level was analyzed by qRT-PCR. NRQ, normalized relative quantity.

muscle (Figure 4A). LTBP4 was shown to be a gene modifier in mdx, sarcoglycanopathies, and DMD patients, where it is associated with fibrogenesis (Flanigan et al., 2013; Heydemann et al., 2009). The expression of LTBP4 by F4/80^{pos} macrophages in fib-mdx muscle was confirmed at the protein level by immunofluorescence. Confocal analysis showed that macrophages expressed both LTBP4 and TGF-β1 in fib-mdx muscle (Figures 4B and S4A). Most (92.5%) of the LTBP4^{pos} cells were F4/80^{pos} cells. Thus, at the protein level, 7.5% of LTBP4-expressing cells were not macrophages and were possibly fibroblasts. qRT-PCR analysis on FACS-isolated populations indicated that FAPs expressed 800-fold more *ltbp4* mRNA than macrophages (Figure S4B). Given that LTBP4 is synthesized as a short or long form under the control of two independent promoters (Kantola et al., 2010), that the long form alone was barely detectable in macrophages, while its expression accounted for 12% of the total *ltbp4* mRNA in FAPs (Figure S4B), and that the antibodies raised against LTBP4 recognize both forms of the protein, we cannot explain the discrepancy between high mRNA and low protein amounts of LTBP4 in FAPs. Thus, we cannot exclude that a LTBP4-latent TGF-β interaction controls TGF-β1 secretion in other cell types such as fibroblastic cells. However, given that LTBPs and TGF-β1 assemble together inside the cell before being secreted in the milieu as a complex (Robertson et al., 2015; Miyazono et al., 1991), only macrophage-derived LTBP4 can control the latency of macrophage-derived TGF-β1.

Three different small interfering RNAs (siRNAs) were used to inhibit *ltbp4* expression in BMDMs from 43% to 56% (Figure 4C). BMDMs treated with fib-mdx muscle homogenates as above (Figure 3D) showed a strongly reduced TGF-β1 secretion when *ltbp4* was silenced (56%–76% inhibition) (Figure 4D). These results indicate that the DMD gene modifier *ltbp4* controlled TGF-β1 secretion in Ly6C^{pos} macrophages in fibrotic muscle.

AMPK Activation Blunts LTBP4 Expression and Latent TGF-β1 Secretion by Ly6C^{pos} Macrophages in fib-mdx

During skeletal muscle regeneration, the transition from pro-inflammatory Ly6C^{pos} macrophages to recovery LyC6^{neg} macrophages is controlled by AMPKα1 activation (Mounier et al., 2013). We therefore investigated whether AMPK activation acted on the LTBP4/TGF-β1 axis in macrophages. We investigated *in vitro* the effects of AMPK activation on BMDMs rendered profibrotic by treatment with fib-mdx muscle homogenates (as in Figure 3F). We showed that AMPK activation by metformin, an antidiabetic compound known to activate AMPK (Foretz et al.,

(B) Confocal analysis (z stack increments of 0.5 μm) of sections of fib-mdx muscles immunolabeled for F4/80 (red), LTBP4 (green), and TGF-β1 (gray); Hoechst (blue). z Stacks are represented for XZ and YZ views along the yellow lines. Scale bar, 50 μm.

(C and D) BMDMs were transfected with three different siRNAs directed against *ltbp4* or with a control siRNA (siScr) and were incubated for 3 days with a fib-mdx muscle extract. (C) *Ltbp4* mRNA level was measured by qRT-PCR and (D) TGF-β1 production was quantitated by ELISA.

Results are means ± SEMs of six (A) and four (C and D) experiments. *$p < 0.05$, **$p < 0.01$, ***$p < 0.001$ between the indicated bars or versus siScr in (C) and (D).

See also Figure S4.

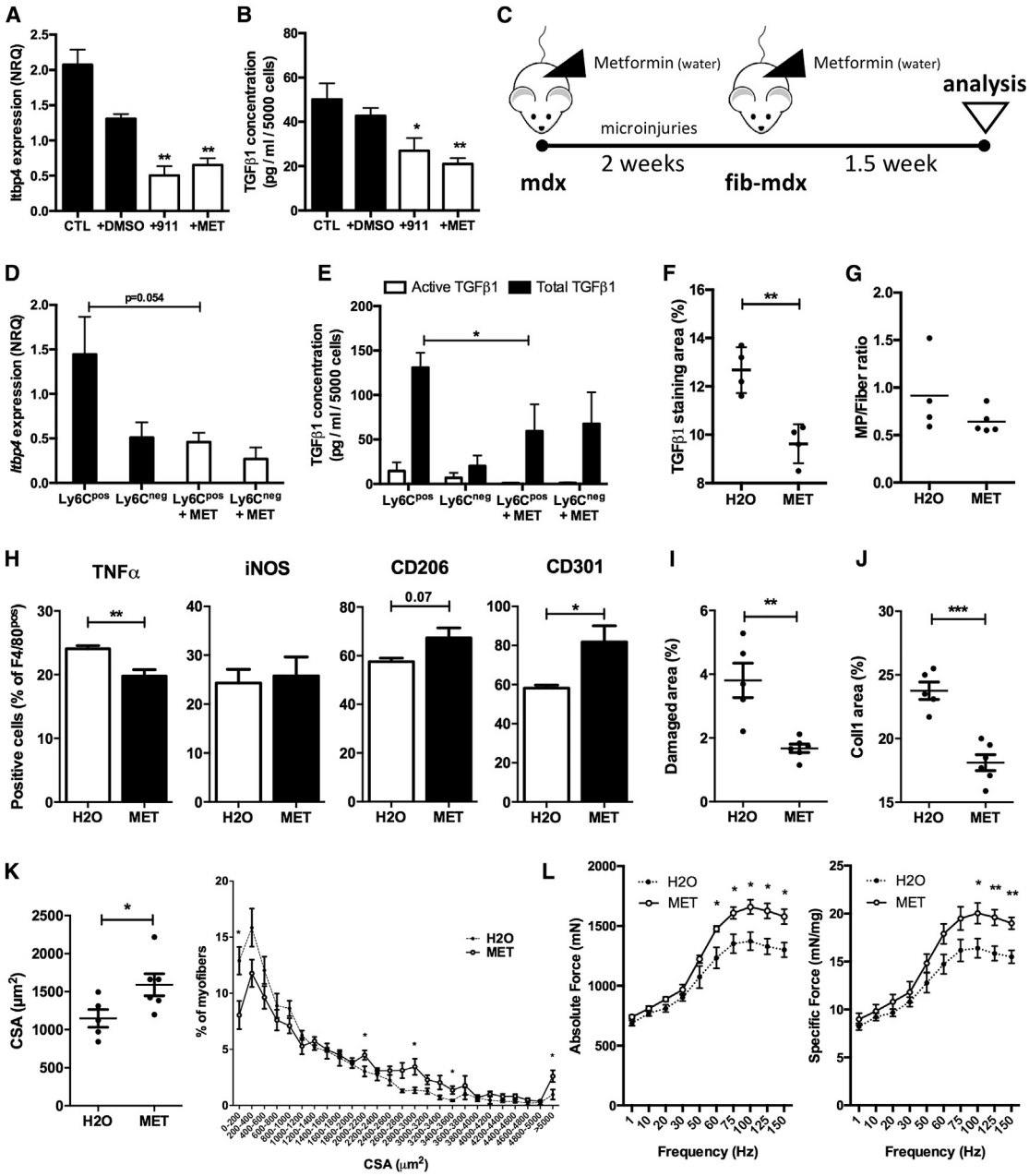

Figure 5. AMPKα1 Activation Regulates Latent TGF-β1 Secretion through the Control of *Itbp4* Expression in Macrophages

(A and B) BMDMs were incubated for 3 days with a fib-mdx muscle extract, and DMSO, 991, or metformin (MET) was added for the last 20 hr. (A) *Ltbp4* expression was measured by qRT-PCR and (B) TGF-β1 production was quantitated by ELISA.

(C) Design of metformin treatment of fib-mdx mice for experiments presented in (D)–(L).

(D) *Ltbp4* expression in macrophage subsets sorted from muscles of treated and non-treated mice was determined by qRT-PCR.

(E) TGF-β1 production by macrophages sorted, as in (D).

(F) Area of TGF-β1 immunolabeling on muscle sections.

(G–K) Histological analysis of muscle sections of treated (MET) and untreated (H_2O) fib-mdx mice.

(G) Number of macrophages (as F4/80^{pos} cells) per fiber.

(H) Percentage of macrophages (as F4/80^{pos} cells) expressing pro- (TNF-α, iNOS) or anti-inflammatory markers (CD301, CD206, Arg1).

(I) Area of necrosis.

(J) Area of collagen I.

(K) Myofiber CSA mean (left graph) and distribution (right graph).

(legend continued on next page)

2014), or by its specific activator 991 (Guigas and Viollet, 2016), strongly reduced *ltbp4* expression by BMDMs treated by fib-mdx muscle homogenates (68% and 61%, respectively) (Figure 5A). In the same conditions, TGF-β1 production by macrophages was strongly reduced upon AMPK activation (58% and 37%, respectively) (Figure 5B). To confirm this circuit of regulation *in vivo*, and since specific activation of AMPK *in vivo* with 991 is not viable, fib-mdx mice were treated with metformin during fibrosis establishment (Figure 5C). Ly6C^{pos} macrophages isolated from these muscles exhibited a strong decrease (68%) in *ltbp4* expression (Figure 5D), associated with a reduction in their TGF-β1 production (55%) (Figure 5E) (note that the weak secretion of active TGF-β1 was also completely blunted upon metformin treatment). Consequently, metformin treatment induced a 25% decrease in TGF-β1 staining in the muscle (Figure 5F), while the number of macrophages did not change (Figure 5G). However, their expression of pro-inflammatory marker TNF-α was decreased and that of anti-inflammatory CD206 (+15%) and CD301 (+41%) markers was increased (Figure 5H). Furthermore, we observed a decrease in the necrotic (−56%) (Figure 5I) and fibrotic (−23%) (Figure 5J) areas in the muscle of the treated animals, together with an increased cross-sectional area (CSA) of the regenerating myofibers (+38%) (Figure 5K), partly due to an increase in the number of myonuclei/myofibers (Figure S5A). Accordingly, the number of Pax7^{pos} cells was decreased upon metformin treatment (Figure S5B), in accordance with a decrease in their self-renewal upon AMPK activation (Theret et al., 2017). Finally, we measured the force produced by the *tibialis anterior* (TA) in these conditions and showed that both absolute and specific isometric force productions were increased in metformin-treated animals (+21% and +22%, respectively) (Figure 5L).

These results show that activation of AMPK dampened *ltbp4* expression by pro-inflammatory macrophages and, consequently, their production of TGF-β1 in the milieu. Therefore, stimulating the shift of pro-inflammatory macrophages toward an anti-inflammatory status is associated with a decrease in fibrosis and an improvement in the muscle in DMD.

Activation of Latent TGF-β1 by FAPs Promotes Fibrosis in fib-mdx

Latent TGF-β1 can be activated by a series of molecules, including enzymes and anchoring proteins such as integrins (Travis and Sheppard, 2014). We isolated FAPs from regenerating, mdx, and fib-mdx muscle and identified that FAPs from fib-mdx exhibited an increased expression of a series of latent TGF-β activators (Figure 6A). Both *matrix metalloproteinase* (*mmp) 14* and *bone morphogenetic protein* (*bmp*) *1* were almost exclusively expressed by FAPs and only weakly by the other cell types in fib-mdx muscle (Figure 6B) (gating strategy is shown in Figures S6A and S6B). These results suggest that FAPs were the main producers of BMP1 and MMP14 to activate latent TGF-β1 previously secreted by Ly6C^{pos} macrophages to promote fibrosis. Expression of both BMP1 and MMP14 by PDGFRα^{pos} cells (i.e., FAPs) (Lemos et al., 2015) was confirmed at the protein level in fib-mdx muscle (Figure 6C). In humans, *bmp1* and *mmp14* were highly expressed by fibroblasts issued from DMD muscle as compared with normal muscle (Figure 6D). Seven-day cultured FAPs did express much lower levels of *bmp1* and *mmp14* than freshly isolated FAPs, indicating that long-term culture of the cells altered some of their properties (Figure S6C). To confirm the functional role of MMP14 and BMP1 produced by fibroblastic cells in the activation of latent TGF-β1, siRNAs were co-transfected in fibroblasts with a collagen I-LUC reporter gene. Fibroblastic *mmp14* or *bmp1* knockdown (Figure 6E) decreased the stimulation of collagen I expression triggered by Ly6C^{pos} macrophages (Figure 6F), demonstrating that these enzymes participated in the activation of latent TGF-β1 produced by fibrotic macrophages. Finally, we treated fib-mdx mice with specific pharmacological inhibitors of MMP14 and BMP1 activities (NSC-405020 and UK-383367, respectively) (Bailey et al., 2008; Zarrabi et al., 2011) and showed a significant improvement in the muscle, including reduction in necrosis (−60% and −57%, respectively) (Figure 6G), reduction in fibrosis (−11% and −8%, respectively) (Figure 6H), and increase in myofiber CSA mean (+20% and +24% respectively, data not shown), and a myofiber CSA distribution shift to larger myofibers (Figure 6I).

DISCUSSION

In the present study, we identified a molecular mechanism of fibrosis establishment in DMD by macrophages. In contrast to their anti-fibroblastic role during skeletal muscle regeneration following acute injury, Ly6C^{pos} macrophages exerted pro-fibrotic activities in dystrophic muscle. These inflammatory macrophages secreted high amounts of latent TGF-β1 due to a high expression of LTBP4, which allows its secretion into the milieu. LTBP4 has been shown to be a gene modifier in DMD patients (Flanigan et al., 2013), and we show here that its expression was controlled by AMPK activation. Consequently, pharmacological activation of AMPK improved the dystrophic muscle. Moreover, latent TGF-β1 was activated by FAPs through a series of enzymes; among these were BMP1 and MMP14, whose specific pharmacological inhibition was also associated with an improvement of dystrophic muscle.

The inflammatory status of macrophages that are responsible for fibrosis is still a matter of debate. Some studies show that anti-inflammatory and alternatively activated macrophages are responsible for fibrosis (Redente et al., 2014; Xue et al., 2015). However, other analyses indicate that CCR2^{pos} or Ly6C^{pos} macrophages drive fibrosis establishment (Baeck et al., 2014; Lebrun et al., 2017), suggesting that depending on the tissue and disease considered, specific macrophage subsets may be involved. In dystrophic skeletal muscle, several studies have implicated macrophages and fibrosis (Vidal et al., 2008; Wehling et al., 2001). However, the role of macrophage-derived TGF-β1

(L) Absolute and specific force measured on TA of fib-mdx and metformin-treated fib-mdx mice. NRQ, normalized relative quantity.
Results are means ± SEMs of three (A), five (B and G–K), four (D–F), and five (L) experiments. *$p < 0.05$, **$p < 0.01$, ***$p < 0.001$ using Student's t test between the indicated bars or versus +DMSO in (A) and (B) or versus H_2O in (K) and (L).
See also Figure S5.

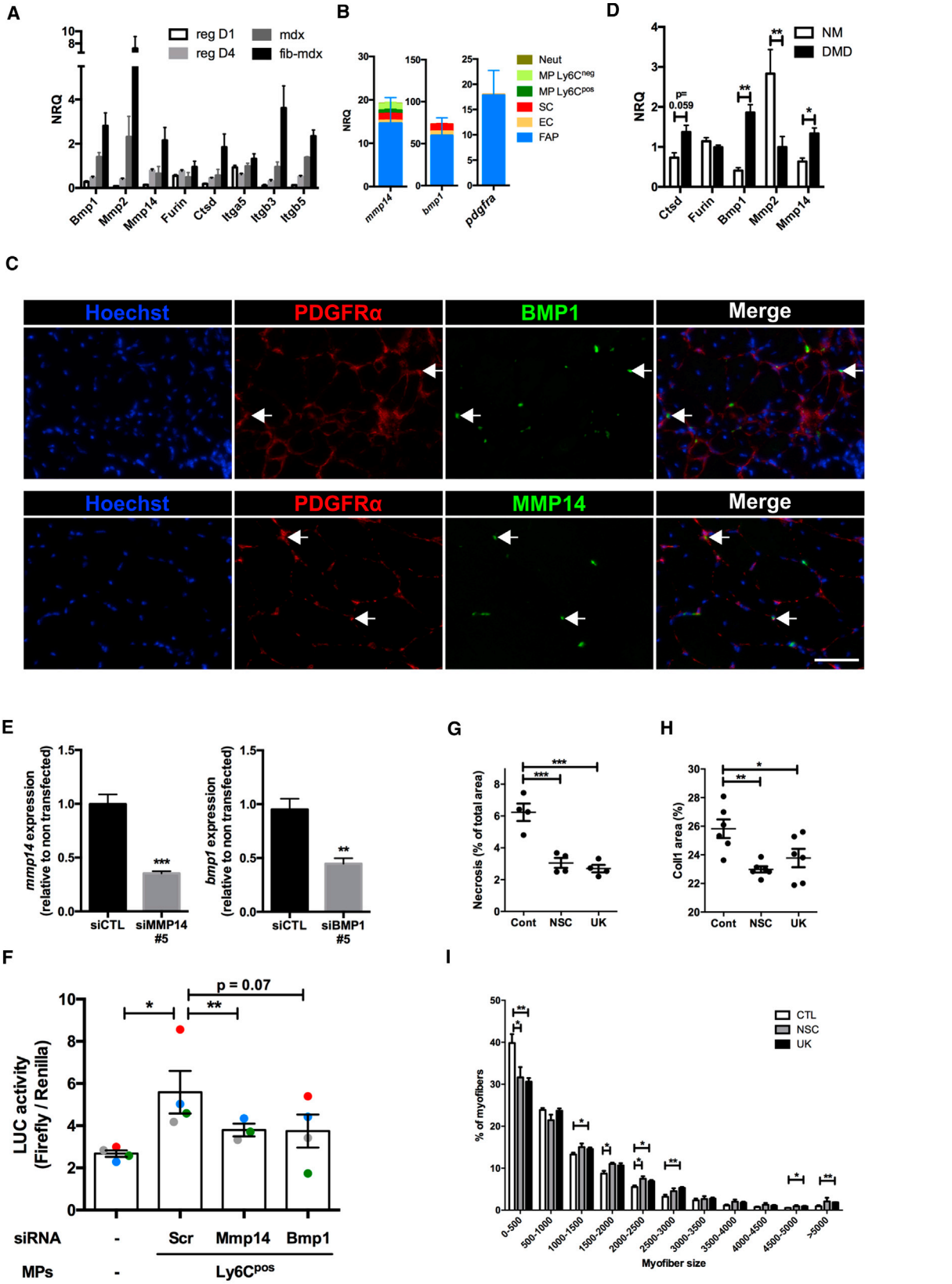

(legend on next page)

has not been addressed, nor has the type of macrophage subset driving fibrosis. Our histological analysis clearly indicates in both murine and human DMD muscle that macrophages expressing pro-inflammatory markers were associated with fibrosis, while, as expected (Arnold et al., 2007; Saclier et al., 2013), areas where myogenesis took place were associated with macrophages expressing anti-inflammatory effectors. These results are in accordance with the beneficial effect on diaphragm fibrosis observed in Toll-like receptor 4 (TLR4)-deficient mdx mice in which pro-inflammatory macrophages are reduced (Giordano et al., 2015). Functionally, Ly6C^{pos} macrophages exerted the opposite effect in regenerating muscle and in fib-mdx. In regenerating muscle, Ly6C^{pos} macrophages inhibited proliferation and differentiation of fibroblasts, and induced their apoptosis, as was previously shown for FAPs (Lemos et al., 2015). Inversely, in fib-mdx, Ly6C^{pos} macrophages promoted the differentiation of fibroblasts along with their production of collagen I, and protected them from apoptosis. The latter two properties were blunted by inhibiting TGF-β1 in the co-culture, indicating the requirement of the profibrotic cytokine in this process. While the secretion of TGF-β1 by macrophages has been known for a long time from seminal *in vitro* and *ex vivo* studies (Assoian et al., 1987; Grotendorst et al., 1989; Khalil et al., 1996), the secretion of TGF-β1 protein by tissue-derived macrophages has been only rarely directly documented (Harel-Adar et al., 2011). The mechanisms regulating *tgfb1* gene expression by macrophages are poorly known, the best characterized being phagocytosis of apoptotic and/or necrotic cells via the phosphatidylserine receptor, which triggers TGF-β1 synthesis (Huynh et al., 2002). Of note, qRT-PCR analysis of sorted Ly6C^{pos} and Ly6C^{neg} macrophage populations indicated no difference in *tgfb1* gene expression, suggesting post-transcriptional regulation to explain different TGF-β1 production by the two populations.

Latent TGF-β1 is secreted from cells within a complex, where it is associated with latent associated peptide (LAP) and LTBP (Miyazono et al., 1991; Robertson et al., 2015). In LTBP4-deficient mice, secretion of TGF-β1 is inhibited, preventing lung fibrosis (Zhou et al., 2009). We showed that in fib-mdx, Ly6C^{pos} macrophages expressed higher levels of *ltbp4* in and that controlled their TGF-β1 secretion, providing a molecular mechanism sustaining the profibrotic activity of Ly6C^{pos} macrophages in muscular dystrophy. LTBP4 is identified as a gene modifier in muscular dystrophies and in DMD patients, specific polymorphisms being associated with different levels of the TGF-β signaling pathway and fibrosis establishment due to differential binding to TGF-β1 and cleavage sensitivity (Flanigan et al., 2013; Heydemann et al., 2009; Lamar et al., 2016).

AMPKα1 is required for the resolution of inflammation and the acquisition of the anti-inflammatory phenotype by macrophages during normal muscle regeneration (Mounier et al., 2013). *In vitro* specific AMPK activation (by 991) in macrophages triggered the downregulation of *ltbp4* expression, which in turn led to a decreased TGF-β1 secretion by these cells. Although AMPK likely controls *ltbp4* expression indirectly, our data show the regulation of TGF-β1 secretion by AMPK activation. As a consequence, *in vivo* pharmacological activation of AMPK by metformin led to an improvement of the dystrophic phenotype, including at the functional level. Although metformin has AMPK-independent properties, improvement of the muscle was associated with a decrease in the pro-inflammatory status and an increase in the anti-inflammatory status of macrophages. Under these conditions, we showed that Ly6C^{pos} macrophages specifically expressed lower levels of *ltbp4* and secreted lower amounts of TGF-β1 *in vivo*. While AMPK activation was shown to reduce fibrosis in several diseases (Jiang et al., 2017) and to improve dystrophic muscle (Ljubicic et al., 2011; Pauly et al., 2012), our data provide evidence of an AMPK-controlled TGF-β1 production by macrophages that can be alleviated through systemic AMPK activation.

Once in the milieu, latent TGF-β1 must be activated to exert its properties and bind to its receptors (Travis and Sheppard, 2014). Activation is made by both enzymatic and mechanical mechanisms. We found that, in fibrotic muscle, FAPs were the main source of TGF-β-activating enzymes, among which MP1 and MMP14, that were also overexpressed by human fibroblasts isolated from human DMD muscle. FACS-sorted FAPs from fib-mdx muscle grew very poorly in culture, however, in contrast to FAPs sorted from non-dystrophic regenerating muscle. This limitation prevented the analysis of their secretion of TGF-β1, as well as their co-culture with macrophages. Nevertheless, we showed that silencing mmp14 or bmp1 in fibroblasts prevented the activation of TGF-β1, and therefore the production of

Figure 6. FAPs Express High Levels of Latent TGF-β Activating Proteases

(A) FAPs were sorted from regenerating (day 1 or 4 after injury) or mdx or fib-mdx muscles, and the mRNA level of various genes coding for activators of latent TGF-β was measured by qRT-PCR.

(B) Neutrophils (Neut), Ly6C^{neg} macrophages (MP Ly6C^{neg}), Ly6C^{pos} macrophages (MP Ly6C^{pos}), satellite cells (SC), endothelial cells (EC), and FAPs were sorted from fib-mdx muscles, and the mRNA levels of *mmp14*, *bmp1*, and *pdgfra* were measured by qRT-PCR.

(C) fib-mdx muscle sections were immunolabeled for MMP14 or BMP1 (green) and PDGFRα (red); Hoechst (blue). Arrows indicate FAPs expressing MMP14 or BMP1. Scale bar, 50 μm.

(D) The mRNA level of several genes coding for activators of latent TGF-β was measured by qRT-PCR in primary human fibroblasts derived from normal muscle (NM) or DMD patient muscle.

(E) NIH 3T3 cells were co-transfected with siRNAs directed against *mmp14* or *bmp1* with a plasmid encoding luciferase under collagen I promoter and *mmp14* (left graph), and *bmp1* (right graph) mRNA level was measured by qRT-PCR. siCTL, control using a non-specific siRNA.

(F) Fibroblasts were transfected as in (E) and were co-cultured with Ly6C^{pos} macrophages sorted from fib-mdx muscle for 20 hr, and luciferase activity was determined. Each color stands for one experiment.

(G–I) fib-mdx mice were treated with pharmacological inhibitors of MMP14 (NSC) or of BMP1 (UK) for 3 weeks. The necrosis area (G), collagen I area (H), and distribution of myofiber CSA (I) were evaluated.

Results are means ± SEMs of three (A, and NM in D), eight (DMD in D), five (E), four (F), and six (G, H, and I) experiments. *$p < 0.05$, **$p < 0.01$, ***$p < 0.001$ using Student's t test.

See also Figure S6.

collagen I when they were co-cultured with Ly6C^{pos} macrophages. Moreover, pharmacological inhibition of either BMP1 or MMP14 improved the fib-mdx phenotype and reduced fibrosis in fib-mdx muscle.

To conclude, the present study evidenced an Ly6C^{pos} profibrotic macrophage subpopulation in dystrophic muscle that exerts its functions by actively producing latent TGF-β1 thanks to the synthesis of LTBP4, which controls its secretion. Latent TGF-β1 is then activated by enzymes produced by FAPs, and the active TGF-β1 acts in turn on FAPs and fibroblastic cells to promote fibrosis (production of collagen I, differentiation into myofibroblasts, protection from apoptosis). Macrophage *ltbp4* expression is reduced by the activation of AMPKα1. Accordingly, this macrophage-FAP fibrotic circuit may be blunted by pharmacological treatments targeting either the production of TGF-β1 by macrophages (via activation of AMPK) or the enzymatic activation of TGF-β1 by FAPs (via inhibition of BMP1 or MMP14), both of which improve dystrophic muscle by reducing necrosis and fibrosis, increasing the size of regenerating myofibers, and increasing muscle strength.

STAR★METHODS

Detailed methods are provided in the online version of this paper and include the following:

- KEY RESOURCES TABLE
- CONTACT FOR REAGENT AND RESOURCE SHARING
- EXPERIMENTAL MODEL AND SUBJECT DETAILS
  - Mice
  - Cells
- METHOD DETAILS
  - Mice experiments
  - Histology and immunofluorescence analyses
  - FACS experiments
  - Cell culture
  - Molecular biology
- QUANTIFICATION AND STATISTICAL ANALYSIS
  - Mouse histology
  - Human histology
  - Statistical Analyses

SUPPLEMENTAL INFORMATION

Supplemental Information includes six figures and two tables and can be found with this article online at https://doi.org/10.1016/j.celrep.2018.10.077.

ACKNOWLEDGMENTS

This work was funded by grants from the Framework Programme FP7 Endostem (under grant agreement 241440), Association Française contre les Myopathies (grant 16029 and MyoNeurAlp Alliance), Fondation pour la Recherche Médicale (Equipe FRM DEQ20140329495), and the Canadian Institutes of Health Research. We thank Peter Mertens (Otto-von-Guericke-Universität, Magdeburg, Germany) for the generous gift of the collagen I-Luc plasmid. We thank the Genom'ic, the Cytometry CyBIO, and the Cellular Imaging facilities of Institut Cochin, Paris, and particularly Thomas Guilbert for building the macros in ImageJ, the Anira-Cytometry facility of SFR Biosciences, Lyon.

AUTHOR CONTRIBUTIONS

Conceptualization, G.J., M.S., and B.C.; Methodology, G.J., M.S., J.G., and B.C.; Validation, G.J., M.S., J.G., R.M., and B.C.; Formal Analysis, G.J., M.S., J.G., and B.C.; Investigation, G.J., M.S., H.Y.-Y., A.K., L.A., C.B., S.B.L., M.M., S.C., M.T., and B.C.; Resources, B.J.P. and I.D.; Writing – Original Draft, G.J., M.S., and B.C.; Writing – Review & Editing, G.J., M.S., B.J.P., R.M., and B.C.; Visualization, G.J., M.S., and B.C.; Supervision, B.C.; Project Administration, B.C. and R.M.; Funding Acquisition, B.C.

DECLARATION OF INTERESTS

The authors declare no competing interests.

Received: January 12, 2018
Revised: September 6, 2018
Accepted: October 19, 2018
Published: November 20, 2018

REFERENCES

Acharyya, S., Villalta, S.A., Bakkar, N., Bupha-Intr, T., Janssen, P.M., Carathers, M., Li, Z.W., Beg, A.A., Ghosh, S., Sahenk, Z., et al. (2007). Interplay of IKK/NF-kappaB signaling in macrophages and myofibers promotes muscle degeneration in Duchenne muscular dystrophy. J. Clin. Invest. *117*, 889–901.

Andreetta, F., Bernasconi, P., Baggi, F., Ferro, P., Oliva, L., Arnoldi, E., Cornelio, F., Mantegazza, R., and Confalonieri, P. (2006). Immunomodulation of TGF-beta 1 in mdx mouse inhibits connective tissue proliferation in diaphragm but increases inflammatory response: implications for antifibrotic therapy. J. Neuroimmunol. *175*, 77–86.

Arnold, L., Henry, A., Poron, F., Baba-Amer, Y., van Rooijen, N., Plonquet, A., Gherardi, R.K., and Chazaud, B. (2007). Inflammatory monocytes recruited after skeletal muscle injury switch into antiinflammatory macrophages to support myogenesis. J. Exp. Med. *204*, 1057–1069.

Assoian, R.K., Fleurdelys, B.E., Stevenson, H.C., Miller, P.J., Madtes, D.K., Raines, E.W., Ross, R., and Sporn, M.B. (1987). Expression and secretion of type beta transforming growth factor by activated human macrophages. Proc. Natl. Acad. Sci. USA *84*, 6020–6024.

Baeck, C., Wei, X., Bartneck, M., Fech, V., Heymann, F., Gassler, N., Hittatiya, K., Eulberg, D., Luedde, T., Trautwein, C., and Tacke, F. (2014). Pharmacological inhibition of the chemokine C-C motif chemokine ligand 2 (monocyte chemoattractant protein 1) accelerates liver fibrosis regression by suppressing Ly-6C(+) macrophage infiltration in mice. Hepatology *59*, 1060–1072.

Bailey, H.H., Attia, S., Love, R.R., Fass, T., Chappell, R., Tutsch, K., Harris, L., Jumonville, A., Hansen, R., Shapiro, G.R., and Stewart, J.A. (2008). Phase II trial of daily oral perillyl alcohol (NSC 641066) in treatment-refractory metastatic breast cancer. Cancer Chemother. Pharmacol. *62*, 149–157.

Biernacka, A., Dobaczewski, M., and Frangogiannis, N.G. (2011). TGF-β signaling in fibrosis. Growth Factors *29*, 196–202.

Chazaud, B. (2014). Macrophages: supportive cells for tissue repair and regeneration. Immunobiology *219*, 172–178.

Chen, Y.W., Nagaraju, K., Bakay, M., McIntyre, O., Rawat, R., Shi, R., and Hoffman, E.P. (2005). Early onset of inflammation and later involvement of TGFbeta in Duchenne muscular dystrophy. Neurology *65*, 826–834.

Desguerre, I., Mayer, M., Leturcq, F., Barbet, J.P., Gherardi, R.K., and Christov, C. (2009). Endomysial fibrosis in Duchenne muscular dystrophy: a marker of poor outcome associated with macrophage alternative activation. J. Neuropathol. Exp. Neurol. *68*, 762–773.

Desguerre, I., Arnold, L., Vignaud, A., Cuvellier, S., Yacoub-Youssef, H., Gherardi, R.K., Chelly, J., Chretien, F., Mounier, R., Ferry, A., and Chazaud, B. (2012). A new model of experimental fibrosis in hindlimb skeletal muscle of adult mdx mouse mimicking muscular dystrophy. Muscle Nerve *45*, 803–814.

Duclos, F., Straub, V., Moore, S.A., Venzke, D.P., Hrstka, R.F., Crosbie, R.H., Durbeej, M., Lebakken, C.S., Ettinger, A.J., van der Meulen, J., et al. (1998).

Progressive muscular dystrophy in alpha-sarcoglycan-deficient mice. J. Cell Biol. *142*, 1461–1471.

Flanigan, K.M., Ceco, E., Lamar, K.M., Kaminoh, Y., Dunn, D.M., Mendell, J.R., King, W.M., Pestronk, A., Florence, J.M., Mathews, K.D., et al.; United Dystrophinopathy Project (2013). LTBP4 genotype predicts age of ambulatory loss in Duchenne muscular dystrophy. Ann. Neurol. *73*, 481–488.

Foretz, M., Guigas, B., Bertrand, L., Pollak, M., and Viollet, B. (2014). Metformin: from mechanisms of action to therapies. Cell Metab. *20*, 953–966.

Geissman, F., Jung, S., and Littman, D.R. (2003). Blood monocytes consist of two principal subsets with distinct migratory properties. Immunity *19*, 71–82.

Giordano, C., Mojumdar, K., Liang, F., Lemaire, C., Li, T., Richardson, J., Divangahi, M., Qureshi, S., and Petrof, B.J. (2015). Toll-like receptor 4 ablation in mdx mice reveals innate immunity as a therapeutic target in Duchenne muscular dystrophy. Hum. Mol. Genet. *24*, 2147–2162.

Grotendorst, G.R., Smale, G., and Pencev, D. (1989). Production of transforming growth factor beta by human peripheral blood monocytes and neutrophils. J. Cell. Physiol. *140*, 396–402.

Guigas, B., and Viollet, B. (2016). Targeting AMPK: from ancient drugs to new small-molecule activators. EXS *107*, 327–350.

Harel-Adar, T., Ben Mordechai, T., Amsalem, Y., Feinberg, M.S., Leor, J., and Cohen, S. (2011). Modulation of cardiac macrophages by phosphatidylserine-presenting liposomes improves infarct repair. Proc. Natl. Acad. Sci. USA *108*, 1827–1832.

Heydemann, A., Ceco, E., Lim, J.E., Hadhazy, M., Ryder, P., Moran, J.L., Beier, D.R., Palmer, A.A., and McNally, E.M. (2009). Latent TGF-beta-binding protein 4 modifies muscular dystrophy in mice. J. Clin. Invest. *119*, 3703–3712.

Huynh, M.L., Fadok, V.A., and Henson, P.M. (2002). Phosphatidylserine-dependent ingestion of apoptotic cells promotes TGF-beta1 secretion and the resolution of inflammation. J. Clin. Invest. *109*, 41–50.

Jiang, S., Li, T., Yang, Z., Yi, W., Di, S., Sun, Y., Wang, D., and Yang, Y. (2017). AMPK orchestrates an elaborate cascade protecting tissue from fibrosis and aging. Ageing Res. Rev. *38*, 18–27.

Joe, A.W., Yi, L., Natarajan, A., Le Grand, F., So, L., Wang, J., Rudnicki, M.A., and Rossi, F.M. (2010). Muscle injury activates resident fibro/adipogenic progenitors that facilitate myogenesis. Nat. Cell Biol. *12*, 153–163.

Kantola, A.K., Ryynänen, M.J., Lhota, F., Keski-Oja, J., and Koli, K. (2010). Independent regulation of short and long forms of latent TGF-beta binding protein (LTBP)-4 in cultured fibroblasts and human tissues. J. Cell. Physiol. *223*, 727–736.

Khalil, N., Corne, S., Whitman, C., and Yacyshyn, H. (1996). Plasmin regulates the activation of cell-associated latent TGF-beta 1 secreted by rat alveolar macrophages after in vivo bleomycin injury. Am. J. Respir. Cell Mol. Biol. *15*, 252–259.

Knipper, J.A., Willenborg, S., Brinckmann, J., Bloch, W., Maaß, T., Wagener, R., Krieg, T., Sutherland, T., Munitz, A., Rothenberg, M.E., et al. (2015). Interleukin-4 receptor α signaling in myeloid cells controls collagen fibril assembly in skin repair. Immunity *43*, 803–816.

Lamar, K.M., Miller, T., Dellefave-Castillo, L., and McNally, E.M. (2016). Genotype-specific interaction of latent TGFβ binding protein 4 with TGFβ. PLoS One *11*, e0150358.

Lapidos, K.A., Kakkar, R., and McNally, E.M. (2004). The dystrophin glycoprotein complex: signaling strength and integrity for the sarcolemma. Circ. Res. *94*, 1023–1031.

Lebrun, A., Lo Re, S., Chantry, M., Izquierdo Carerra, X., Uwambayinema, F., Ricci, D., Devosse, R., Ibouraadaten, S., Brombin, L., Palmai-Pallag, M., et al. (2017). CCR2+ monocytic-myeloid-derived immunosuppressive cells (M-MDSC) inhibit collagen degradation and promote lung fibrosis by producing TGF-beta1. J. Pathol *243*, 320–330.

Lemos, D.R., Babaeijandaghi, F., Low, M., Chang, C.K., Lee, S.T., Fiore, D., Zhang, R.H., Natarajan, A., Nedospasov, S.A., and Rossi, F.M. (2015). Nilotinib reduces muscle fibrosis in chronic muscle injury by promoting TNF-mediated apoptosis of fibro/adipogenic progenitors. Nat. Med. *21*, 786–794.

Ljubicic, V., Miura, P., Burt, M., Boudreault, L., Khogali, S., Lunde, J.A., Renaud, J.M., and Jasmin, B.J. (2011). Chronic AMPK activation evokes the slow, oxidative myogenic program and triggers beneficial adaptations in mdx mouse skeletal muscle. Hum. Mol. Genet. *20*, 3478–3493.

Minutti, C.M., Jackson-Jones, L.H., García-Fojeda, B., Knipper, J.A., Sutherland, T.E., Logan, N., Ringqvist, E., Guillamat-Prats, R., Ferenbach, D.A., Artigas, A., et al. (2017). Local amplifiers of IL-4Rαmediated macrophage activation promote repair in lung and liver. Science *356*, 1076–1080.

Misharin, A.V., Morales-Nebreda, L., Reyfman, P.A., Cuda, C.M., Walter, J.M., McQuattie-Pimentel, A.C., Chen, C.I., Anekalla, K.R., Joshi, N., Williams, K.J.N., et al. (2017). Monocyte-derived alveolar macrophages drive lung fibrosis and persist in the lung over the life span. J. Exp. Med. *214*, 2387–2404.

Miyazono, K., Olofsson, A., Colosetti, P., and Heldin, C.H. (1991). A role of the latent TGF-beta 1-binding protein in the assembly and secretion of TGF-beta 1. EMBO J. *10*, 1091–1101.

Mojumdar, K., Liang, F., Giordano, C., Lemaire, C., Danialou, G., Okazaki, T., Bourdon, J., Rafei, M., Galipeau, J., Divangahi, M., and Petrof, B.J. (2014). Inflammatory monocytes promote progression of Duchenne muscular dystrophy and can be therapeutically targeted via CCR2. EMBO Mol. Med. *6*, 1476–1492.

Mounier, R., Théret, M., Arnold, L., Cuvellier, S., Bultot, L., Göransson, O., Sanz, N., Ferry, A., Sakamoto, K., Foretz, M., et al. (2013). AMPKα1 regulates macrophage skewing at the time of resolution of inflammation during skeletal muscle regeneration. Cell Metab. *18*, 251–264.

Pauly, M., Daussin, F., Burelle, Y., Li, T., Godin, R., Fauconnier, J., Koechlin-Ramonatxo, C., Hugon, G., Lacampagne, A., Coisy-Quivy, M., et al. (2012). AMPK activation stimulates autophagy and ameliorates muscular dystrophy in the mdx mouse diaphragm. Am. J. Pathol. *181*, 583–592.

Pessina, P., Kharraz, Y., Jardí, M., Fukada, S., Serrano, A.L., Perdiguero, E., and Muñoz-Cánoves, P. (2015). Fibrogenic cell plasticity blunts tissue regeneration and aggravates muscular dystrophy. Stem Cell Reports *4*, 1046–1060.

Redente, E.F., Keith, R.C., Janssen, W., Henson, P.M., Ortiz, L.A., Downey, G.P., Bratton, D.L., and Riches, D.W. (2014). Tumor necrosis factor-α accelerates the resolution of established pulmonary fibrosis in mice by targeting profibrotic lung macrophages. Am. J. Respir. Cell Mol. Biol. *50*, 825–837.

Robertson, I.B., Horiguchi, M., Zilberberg, L., Dabovic, B., Hadjiolova, K., and Rifkin, D.B. (2015). Latent TGF-β-binding proteins. Matrix Biol. *47*, 44–53.

Rosenberg, A.S., Puig, M., Nagaraju, K., Hoffman, E.P., Villalta, S.A., Rao, V.A., Wakefield, L.M., and Woodcock, J. (2015). Immune-mediated pathology in Duchenne muscular dystrophy. Sci. Transl. Med. *7*, 299rv4.

Saclier, M., Yacoub-Youssef, H., Mackey, A.L., Arnold, L., Ardjoune, H., Magnan, M., Sailhan, F., Chelly, J., Pavlath, G.K., Mounier, R., et al. (2013). Differentially activated macrophages orchestrate myogenic precursor cell fate during human skeletal muscle regeneration. Stem Cells *31*, 384–396.

Schneider, C.A., Rasband, W.S., and Eliceiri, K.W. (2012). NIH Image to ImageJ: 25 years of image analysis. Nat. Methods *9*, 671–675.

Tacke, F., and Zimmermann, H.W. (2014). Macrophage heterogeneity in liver injury and fibrosis. J. Hepatol. *60*, 1090–1096.

Theret, M., Gsaier, L., Schaffer, B., Juban, G., Ben Larbi, S., Weiss-Gayet, M., Bultot, L., Collodet, C., Foretz, M., Desplanches, D., et al. (2017). AMPKα1-LDH pathway regulates muscle stem cell self-renewal by controlling metabolic homeostasis. EMBO J. *36*, 1946–1962.

Travis, M.A., and Sheppard, D. (2014). TGF-β activation and function in immunity. Annu. Rev. Immunol. *32*, 51–82.

Uezumi, A., Fukada, S., Yamamoto, N., Takeda, S., and Tsuchida, K. (2010). Mesenchymal progenitors distinct from satellite cells contribute to ectopic fat cell formation in skeletal muscle. Nat. Cell Biol. *12*, 143–152.

Varga, T., Mounier, R., Horvath, A., Cuvellier, S., Dumont, F., Poliska, S., Ardjoune, H., Juban, G., Nagy, L., and Chazaud, B. (2016a). Highly dynamic transcriptional signature of distinct macrophage subsets during sterile inflammation, resolution, and tissue repair. J. Immunol. *196*, 4771–4782.

Varga, T., Mounier, R., Patsalos, A., Gogolák, P., Peloquin, M., Horvath, A., Pap, A., Daniel, B., Nagy, G., Pintye, E., et al. (2016b). Macrophage PPARγ,

a lipid activated transcription factor controls the growth factor GDF3 and skeletal muscle regeneration. Immunity *45*, 1038–1051.

Vetrone, S.A., Montecino-Rodriguez, E., Kudryashova, E., Kramerova, I., Hoffman, E.P., Liu, S.D., Miceli, M.C., and Spencer, M.J. (2009). Osteopontin promotes fibrosis in dystrophic mouse muscle by modulating immune cell subsets and intramuscular TGF-beta. J. Clin. Invest. *119*, 1583–1594.

Vidal, B., Serrano, A.L., Tjwa, M., Suelves, M., Ardite, E., De Mori, R., Baeza-Raja, B., Martínez de Lagrán, M., Lafuste, P., Ruiz-Bonilla, V., et al. (2008). Fibrinogen drives dystrophic muscle fibrosis via a TGFbeta/alternative macrophage activation pathway. Genes Dev. *22*, 1747–1752.

Villalta, S.A., Nguyen, H.X., Deng, B., Gotoh, T., and Tidball, J.G. (2009). Shifts in macrophage phenotypes and macrophage competition for arginine metabolism affect the severity of muscle pathology in muscular dystrophy. Hum. Mol. Genet. *18*, 482–496.

Villalta, S.A., Rinaldi, C., Deng, B., Liu, G., Fedor, B., and Tidball, J.G. (2011). Interleukin-10 reduces the pathology of mdx muscular dystrophy by deactivating M1 macrophages and modulating macrophage phenotype. Hum. Mol. Genet. *20*, 790–805.

Wehling, M., Spencer, M.J., and Tidball, J.G. (2001). A nitric oxide synthase transgene ameliorates muscular dystrophy in mdx mice. J. Cell Biol. *155*, 123–131.

Wynn, T.A., and Vannella, K.M. (2016). Macrophages in tissue repair, regeneration, and fibrosis. Immunity *44*, 450–462.

Xue, J., Sharma, V., Hsieh, M.H., Chawla, A., Murali, R., Pandol, S.J., and Habtezion, A. (2015). Alternatively activated macrophages promote pancreatic fibrosis in chronic pancreatitis. Nat. Commun. *6*, 7158.

Zarrabi, K., Dufour, A., Li, J., Kuscu, C., Pulkoski-Gross, A., Zhi, J., Hu, Y., Sampson, N.S., Zucker, S., and Cao, J. (2011). Inhibition of matrix metalloproteinase 14 (MMP-14)-mediated cancer cell migration. J. Biol. Chem. *286*, 33167–33177.

Zhou, Y., Koli, K., Hagood, J.S., Miao, M., Mavalli, M., Rifkin, D.B., and Murphy-Ullrich, J.E. (2009). Latent transforming growth factor-beta-binding protein-4 regulates transforming growth factor-beta1 bioavailability for activation by fibrogenic lung fibroblasts in response to bleomycin. Am. J. Pathol. *174*, 21–33.

STAR★METHODS

KEY RESOURCES TABLE

REAGENT or RESOURCE	SOURCE	IDENTIFIER
Antibodies		
Rat monoclonal anti-F4/80 (clone CI:A3-1)	Abcam	Cat# ab6640; RRID:AB_1140040
Rat monoclonal anti-F4/80	Abcam	Cat# ab74383; RRID:AB_1860121
Goat polyclonal anti-Arg1	Santa Cruz Biotechnology	Cat# sc-18355; RRID:AB_2058957
Rabbit polyclonal anti-CCL3	Abcam	Cat# ab32609; RRID:AB_776125
Rabbit monoclonal anti-CCR2 (clone E68)	Abcam	Cat# ab32144; RRID:AB_1603737
Rat monoclonal anti-CD206 (clone MR5D3)	Santa Cruz Biotechnology	Cat# sc-58987; RRID:AB_2144905
Rat monoclonal anti-CD301 (clone ER-MP23),	Abcam	Cat# ab59167; RRID:AB_941058
Rabbit polyclonal anti-Collagen I	Abcam	Cat# ab292; RRID:AB_303415
Rabbit polyclonal anti-Collagen I	Abcam	Cat# ab34710; RRID:AB_731684
Goat polyclonal anti-Collagen I	Southern Biotech	Cat# 1310-01
Goat polyclonal anti-Cox2 (ab23672),	Abcam	Cat# ab23672; RRID:AB_731725
Rat monoclonal anti-Dectin 1 (clone 2A11),	Abcam	Cat# ab53427; RRID:AB_2040609
Rabbit polyclonal anti-IL-10	Abcam	Cat# ab9969; RRID:AB_308826
Rabbit polyclonal anti-iNOS	Abcam	Cat# ab15323; RRID:AB_301857
Rabbit polyclonal anti-BMP1	Abcam	Cat# ab118520; RRID:AB_10899275
Rat monoclonal anti-Laminin (clone AL-1),	Abcam	Cat# ab78287; RRID:AB_1604106
Rabbit polyclonal anti-Laminin	Sigma-Aldrich	Cat# L9393; RRID:AB_477163
Goat polyclonal anti-PDGFRα	R&D Systems	Cat# AF1062; RRID:AB_2236897
Rabbit polyclonal anti-TNFα	Abcam	Cat# ab34839; RRID:AB_778527
Rabbit polyclonal anti-LTBP4	Santa Cruz Biotechnology	Cat# sc-33144; RRID:AB_2139064
Rabbit monoclonal anti-MMP14 (clone EP1264Y)	Abcam	Cat# ab51074; RRID:AB_881234
Donkey anti-rat IgG (H+L), Cy3-conjugated	Jackson ImmunoResearch	Cat# 712-165-153; RRID:AB_2340667
Donkey anti-rabbit IgG (H+L), Cy3-conjugated	Jackson ImmunoResearch	Cat# 711-165-152; RRID:AB_2307443
Donkey anti-rabbit IgG (H+L), FITC-conjugated	Jackson ImmunoResearch	Cat# 711-095-152; RRID:AB_2315776
Donkey anti-goat IgG (H+L), Cy3-conjugated	Jackson ImmunoResearch	Cat# 705-165-147; RRID:AB_2307351
Donkey anti-goat IgG (H+L), FITC-conjugated	Jackson ImmunoResearch	Cat# 705-095-147; RRID:AB_2340401
Donkey anti-mouse IgG (H+L), Cy3-conjugated	Jackson ImmunoResearch	Cat# 715-165-150; RRID:AB_2340813
Donkey anti-mouse IgG (H+L), FITC-conjugated	Jackson ImmunoResearch	Cat# 715-095-150; RRID:AB_2340792
Donkey anti-mouse IgG (H+L), DyLight649-conjugated	Jackson ImmunoResearch	Cat# 715-495-150
Mouse monoclonal anti-CD68 (Clone KP1),	Abcam	Cat# ab955; RRID:AB_307338
Mouse monoclonal anti-Myogenin	DSHB	Cat# F5D; RRID:AB_528355
Mouse monoclonal anti-eMHC	DSHB	Cat# F1.652; RRID:AB_528358
Rat monoclonal anti-mouse CD16/CD32 (clone 2.4G2)	BD Biosciences	Cat# 553142; RRID:AB_394657
Rat monoclonal anti-Ly6C/G (clone RB6-8C5), APC-conjugated	Thermo Fisher Scientific	Cat# 17-5931-82; RRID:AB_469476
Mouse monoclonal anti-CD64 (Clone X54-5/7.1), AF647-conjugated	BD Biosciences	Cat# 558539; RRID:AB_647120
Rat monoclonal anti-F4/80 (clone BM8), PE-conjugated	Thermo Fisher Scientific	Cat# 12-4801-82; RRID:AB_465923
Rat monoclonal anti-CD45 (clone 30-F11), PE-Cy7-conjugated	Thermo Fisher Scientific	Cat# 25-0451-82; RRID:AB_2734986
Rat monoclonal anti-Ly6C (clone HK1.4), APC-conjugated	Thermo Fisher Scientific	Cat# 17-5932-82; RRID:AB_1724153
Rat monoclonal anti-Sca-1 (clone D7), PerCP-Cy5.5-conjugated	Thermo Fisher Scientific	Cat# 45-5981-82; RRID:AB_914372

(*Continued on next page*)

Continued

REAGENT or RESOURCE	SOURCE	IDENTIFIER
Rat monoclonal anti-α7-integrin (clone R2F2), AF647-conjugated	AbLab	Cat# 67-0010-05
Rat monoclonal anti-CD31 (clone 390), PE-conjugated	Thermo Fisher Scientific	Cat# 12-0311-82; RRID:AB_465632
Rat monoclonal anti-CD34 (clone RAM34), FITC-conjugated	Thermo Fisher Scientific	Cat# 11-0341-82; RRID:AB_465021
Mouse monoclonal anti-α-SMA (clone 1A4)	Sigma-Aldrich	Cat# A5228; RRID:AB_262054
Rabbit polyclonal anti-Ki67	Abcam	Cat# ab15580; RRID:AB_443209
Rabbit polyclonal anti-active Caspase 3	Abcam	Cat# ab13847; RRID:AB_443014
Mouse monoclonal blocking anti-TGFβ1 (clone 2Ar2)	Abcam	Cat# ab64715; RRID:AB_1144265
Biological Samples		
Fibroblasts from human muscle	Cochin Hospital Cell Bank, Paris, agreement no. DC-2009-944 (Desguerre et al., 2009 PMID 19535995).	N/A
Human muscle biopsies	(Desguerre et al., 2009 PMID 19535995)	N/A
Chemicals, Peptides, and Recombinant Proteins		
Compound 991	SpiroChem	CAS:129739-36-2
Cardiotoxin from Naja pallida	Latoxan	Cat# L8102
Collagenase B	Roche Diagnostics GmbH	Cat# 11088831001
Dispase II	Roche Diagnostics GmbH	Cat# 04942078001
DMEM/F-12 medium, Glutamax Supplement	GIBCO	Cat# 31331028
DMEM, high glucose, Glutamax Supplement, pyruvate	GIBCO	Cat# 31966021
DMSO	Sigma-Aldrich	Cat# D2650; CAS:67-68-5
Fetal Bovine Serum (FBS)	GIBCO	Cat# 10270106
jetPRIME®	Polyplus transfection	Cat# 114-01
LightCycler® 480 SYBR Green I Master	Roche Diagnostics	Cat# 04887352001
Lipofectamine 2000	Invitrogen	Cat# 11668500
Metformin hydrochloride	Sigma-Aldrich	Cat# PHR1084; CAS:1115-70-4
NSC-405020	MedChemExpress	Cat# HY-15827; CAS:7497-07-6
Recombinant Mouse IFNγ	R&D Systems	Cat# 485-MI-100; GenPept: P01580
Recombinant Mouse IL4	R&D Systems	Cat# 404-ML-010 ; Genpept: P07750
RNeasy Plus Micro kit	QIAGEN	Cat# 74034
TRIzol® Reagent	Life Technologies	Cat# 15596018
UK-383367	Sigma-Aldrich	Cat# PZ0156; CAS:348622-88-8
Critical Commercial Assays		
Dual-Glo Luciferase Assay System	Promega	Cat# E2920
TGF beta-1 Human/Mouse Uncoated ELISA Kit	Thermo Fisher Scientific	Cat# 88-8350-22
Experimental Models: Cell Lines		
NIH 3T3 cell line	ECACC	Cat# 93061524; RRID: CVCL_0594
L929 cell line	ECACC	Cat# 85011425; RRID: CVCL_0462
Experimental Models: Organisms/Strains		
Mouse C57BL/6J	Jaxmice	Cat# 000664; RRID_IMSR_JAX:000664
Mouse CX3CR1$^{GFP/+}$ (Cx3cr1^{tm1Litt}/+). Mice were backcrossed for ten generations to C57BL/6 mice as described in Geissman et al., 2003 (PMID:12871640)	TAAM Orleans, CNRS	RRID:MGI:4833984
Mouse mdx (Dmd$^{mdx-4cv}$/Dmd$^{mdx-4cv}$)	Jaxmice	Cat# 002378 RRID:MGI:3798618
Mouse sgca$^{-/-}$ (Sgca^{tm1Kcam}/ Sgca^{tm1Kcam}). Mice were backcrossed for ten generations to C57BL/6 mice .	MGI	RRID:MGI:2176866

(*Continued on next page*)

Continued

REAGENT or RESOURCE	SOURCE	IDENTIFIER
Oligonucleotides		
AllStars Negative Control siRNA	QIAGEN	Cat# 1027280
Ltbp4 siRNA#1 (Mm_Ltbp4_4);	QIAGEN	Cat# SI 00244160
Ltbp4 siRNA#2 (Mm_Ltbp4_7);	QIAGEN	Cat# SI 02748095
Ltbp4 siRNA#3 (Mm_Ltbp4_8);	QIAGEN	Cat# SI 04942623
Mmp14 siRNA#5 (Mm_Mmp14_5);	QIAGEN	Cat# SI 02687713
Bmp1 siRNA#5 (Mm_Bmp1_5);	QIAGEN	Cat# SI 02669457
Primers (*cf.* Table S2)	Eurogentec	N/A
Recombinant DNA		
pGL3-Basic control plasmid	Promega	Cat# E1751
pGl3-Collagen I plasmid	Peter Mertens, Otto-von-Guericke-Universität Magdeburg, Germany	N/A
pRL-TK Renilla Luciferase Control Reporter Vector	Promega	Cat# E2241
Software and Algorithms		
ImageJ	Schneider et al., 2012; PMID: 22930834	https://imagej.net/Welcome
GraphPad Prism	GraphPad Software	https://www.graphpad.com/scientific-software/prism/

CONTACT FOR REAGENT AND RESOURCE SHARING

Further information and requests for reagents may be directed to, and will be fulfilled by the Lead Contact, Bénédicte Chazaud (benedicte.chazaud@inserm.fr).

EXPERIMENTAL MODEL AND SUBJECT DETAILS

Mice

C57BL/6, CX3CR1$^{GFP/+}$, mdx, mdx;CX3CR1$^{GFP/+}$, sgca$^{+/-}$, sgca$^{-/-}$, sgca$^{+/-}$;CX3CR1$^{GFP/+}$ and sgca$^{-/-}$;CX3CR1$^{GFP/+}$ mice were bred and used according to French and European regulations. The protocols have been approved by the Ethical committee from Université Paris Descartes (CEEA34.BC-RM.053.12) and from Université Claude Bernard Lyon 1 (CEEA55 APAFIS#5871-2016062912432608 v2). Experiments were conducted on males at 8-10 weeks of age for mdx and 16-18 weeks of age for sgca. Muscle injury was caused by intramuscular injection of cardiotoxin in the Tibialis Anterior (TA) muscle, as previously described (Mounier et al., 2013). Fib-mdx was realized as previously described (Desguerre et al., 2012) and mice were studied one week after the last injuries.

Cells

Mouse cell line

NIH 3T3 cells were cultured in DMEM Glutamax (GIBCO) containing 15% Fetal Bovine Serum (FBS) (GIBCO).

Primary Mouse cells: Bone Marrow Derived Macrophages (BMDM).

Total mouse bone marrow was obtained by flushing femur and tibiae with DMEM and cells were cultured in DMEM containing 20% Fetal Bovine Serum (FBS) and 30% of L929 cell line-derived conditioned medium (enriched in CSF-1) for 6-7 days.

Primary Mouse cells: freshly FACS-isolated macrophages

Macrophages were isolated from skeletal TA muscle and directly used for coculture experiments (see below).

Primary Human cells: fibroblasts from human muscle

were obtained from DMD or non-DMD patients, as described in (Desguerre et al., 2009) from Cochin Hospital Cell Bank, Paris, agreement no. DC-2009-944.

Human muscle

Muscle biopsies from 6 patients with DMD, whose diagnosis was established based on a total absence of dystrophin (negative Dys1, Dys2, and Dys3 by immunohistochemistry and confirmed by western blot), were used as in (Desguerre et al., 2009).

METHOD DETAILS

Mice experiments

Mice treatments

Metformin (Sigma) was added in the drinking water (200 mg/kg/day, i.e., 1 mg/ml, replaced every day) during the 2 weeks of fibrosis establishment in the fib-mdx model and for further 1.5 week. MMP14 inhibitor (NSC-405020, MedChemExpress) and BMP1 inhibitor (UK-383367, Sigma-Aldrich) were solubilized in PBS containing 5% DMSO and were injected (i.p., 10 mg/kg for NSC-405020 and 4 mg/kg for UK-383367) every 3 days during the 2 weeks of fibrosis establishment in the fib-mdx model and for 1 more week.

In vivo *isometric force measurement*

Mice were maintained under isoflurane anesthesia. A small transverse incision was made above the right malleoli in order to expose all the tendons surrounding the ankle joint. All the tendons except that of TA muscle were severed to specifically assess the isometric force produced by this muscle. Skin incision was closed using 5/0 polyester fiber suture. Each mouse was then placed supine in a cradle allowing for a standardization of the animal positioning. The right foot was positioned and firmly immobilized through a rigid slipper on a pedal of an ergometer (NIMPHEA_Research, AII Biomedical SAS). The pedal of the ergometer was adjusted to position the ankle joint at 20° of plantar flexion (where 0° corresponding to the pedal of the ergometer perpendicular to the tibia). The right knee was also firmly maintained using a rigid fixation in order to optimize isometric force recordings. Two 27G needle electrodes (745 12-100/24, Ambu® Neuroline) were positioned subcutaneously on the proximal and distal parts of the TA. Monophasic rectangular pulses of 0.2 ms were delivered using a constant-current stimulator (Digitimer DS7AH, Hertfordshire, UK; maximal voltage: 400 V). The force-frequency curves were determined by stepwise increasing stimulation frequency, with resting periods > 30 s between stimuli in order to avoid effects due to fatigue. Force signal was sampled at 1000 Hz using a Powerlab system and Labchart software (ADinstruments).

Histology and immunofluorescence analyses

Mouse

Fascia of TA muscles was removed, then muscles were frozen in nitrogen-chilled isopentane and kept at −80°C until use. 8 μm-thick cryosections were prepared for hematoxylin-eosin (HE), masson trichrome (MT) and immunolabelings. For double immunolabelings, cryosections were labeled with antibodies (from Abcam unless indicated) against F4/80 (ab6640, ab74383) overnight at 4°C and labeling using the second antibody was performed for 2 h at 37°C. Antibodies were directed against Arginase 1 (sc-18355, Santa Cruz), CCL3 (ab32609), CCR2 (ab32144), CD206 (sc-58987, Santa Cruz), CD301 (ab59167), Collagen I (ab292, ab34710 or Biotech 131001), Cox2 (ab23672), Dectin 1 (ab53427), IL-10 (ab9969), iNOS (ab15323), Laminin (L9393, sigma aldrich, or ab78287), PDGFRα (AF1062, R&D System), TNFα (ab34839), LTBP4 (sc-33144, Santa Cruz), MMP14 (ab51074) and BMP1 (ab118520). Secondary antibodies were coupled to FITC, Cy3 or Cy5 (Jackson Immunoresearch Inc). Muscle stem cells were immunolabeled with an antibody directed against Pax7 as previously described (Theret et al., 2017).

Human

Serial muscle sections were immunolabelled as described above using the following antibodies CD68 (ab955), Myogenin (Developmental Studies Hybridoma Bank, DSHB F5D), eMHC (DSHB F1.652), Collagen 1 (Southern Biotech), CD163 (sc-20066), CD206 (ab64693), Arg1 (sc-18355), iNOS (ab15323), TNFα (ab6671) and revealed with Cy3- and FITC- conjugated secondary antibodies (antibody combinations are shown in Table S1).

FACS experiments

Isolation of macrophages from skeletal muscle

Fascia of the TA muscles was removed. Muscles were dissociated and digested in RPMI medium containing collagenase B 2 mg/ml (Roche Diagnostics GmbH) at 37°C for 1h (2h for fibrotic muscle) and passed through a 30 μm cell strainer (Miltenyi Biotec). $CD45^{pos}$ cells were isolated using magnetic sorting (Miltenyi Biotec) and incubated with anti-mouse FcγRII/III (2.4G2) for 20 min at 4°C in PBS 2% FBS. Cells were then stained with APC-conjugated anti-Ly6C/G or anti-Ly6C antibodies (eBioscience) and/or CD64 (BD PharMingen 558539) for 30 min at 4°C. Macrophages were analyzed with a Fortessa flow cytometer (BD Biosciences) or were sorted using a FACS Aria III cell sorter (BD Biosciences). Analyses of immune cell population were done using antibodies against CD11b, CD3, CD11c, MgI1, Ly6C, LyC6G, NK1.1 (BD biosciences) and F4/80 (ebiosciences) (gating strategy is shown Figure S1).

Isolation of all cell populations from skeletal muscle

TA muscles were dissociated and digested in DMEM F/12 medium (GIBCO) containing 10 mg/ml of collagenase B and 2.4 U/ml Dispase (Roche Diagnostics GmBH) at 37°C for 30 min (1h for fibrotic muscles) and passed through a 30 μm cell strainer. $CD45^{pos}$ and $CD45^{neg}$ were separated using magnetic beads. $CD45^{pos}$ cells were incubated with anti-mouse FcγRII/III (2.4G2) for 20 min at 4°C in PBS 2% FBS and stained with PE-Cy7-conjugated anti-CD45 (25-0451-82, eBioscience) and APC-conjugated anti-Ly6C antibody (17-5932-82, eBioscience) for 30 min at 4°C. $CD45^{neg}$ cells were stained with PE-Cy7-conjugated anti-CD45, PerCP-Cy5.5-conjugated anti-Sca-1 (45-5981-82, eBioscience), Alexa Fluor 647-conjugated anti-α7-integrin (AB0000538, AB lab, University British Columbia), PE-conjugated anti-CD31 (12-0311-82, eBioscience) and FITC-conjugated anti-CD34 (11-0341-82, eBioscience) antibodies for 30 min at 4°C. Cells were sorted using a FACS Aria II cell sorter (BD Biosciences). Flow cytometry plots and gating strategy are provided in Figure S6A and S6B.

Cell culture

Bone Marrow Derived Macrophages (BMDM).

Total mouse bone marrow was obtained by flushing femur and tibiae with DMEM and cells were cultured in DMEM containing 20% Fetal Bovine Serum (FBS) and 30% of L929 cell line-derived conditioned medium (enriched in CSF-1) for 6-7 days. Macrophages were polarized toward various inflammatory states using 50 ng/ml IFNγ (M1), 10 ng/ml IL4 (M2a) or 1 μg/ml of total protein lysate from Fib-mdx muscle, in DMEM containing 10% FBS for 3 days. In some experiments, DMSO, 10 μM 991 (SpiroChem) or 1 mM Metformin was added to the culture medium for the last 20 h. When required, control siRNAs (AllStars Negative Control siRNA, QIAGEN) or siRNAs directed against *ltbp4* (GeneSolution siRNA, QIAGEN) were transfected into BMDM (10 nM final concentration) using jetPRIME® (Polyplus transfection) for 4-6 hours. Medium was then washed with PBS and transfected BMDM were polarized as described above.

Coculture of macrophages with fibroblasts

NIH 3T3 cells were cultured in DMEM Glutamax (GIBCO) containing 15% Fetal Bovine Serum (FBS) (GIBCO). For the Collagen-1 luciferase assay, NIH 3T3 were seeded at 28000 cells/cm^2 in 96 well-plates. The next day, cells were co-transfected with Lipofectamine 2000 (Promega) and incubated with 1.6 μg of pGl3-Collagen I plasmid (luciferase under the collagen I promoter, a generous gift of Peter Mertens, Otto-von-Guericke-Universität Magdeburg, Germany) or pGl3-control plasmid. In some experiments, NIH 3T3 cells were co-transfected with pGL3-Collagen I (0.5 μg), 0.5 μg of pRL-TK (0.5 μg) (Renilla Luciferase Control Reporter Vectors, Promega) and 10 nM of control siRNAs (AllStars Negative Control siRNA, QIAGEN) or siRNAs directed against *mmp14* or *bmp1* (GeneSolution siRNA, QIAGEN) using Jetprime (Polyplus transfection) for 4h. Medium was removed and cells were cocultured overnight with sorted macrophages (14000 cell/cm^2) in DMEM Glutamax containing 1% FBS. Cocultures were rinsed with PBS and cells were processed for Dual-Glo Luciferase Assay System (Promega) and quantified with a Luminometer. For the analysis of proliferation, differentiation and apoptosis of fibroblasts, NIH 3T3 cells were seeded at 10000 cells/cm^2 in 96 well-plates and cocultured overnight with sorted macrophages (10000 cells/cm^2) in DMEM Glutamax containing 1% FBS. In some experiments, blocking anti-TGFβ1 antibodies were added (1/200, Abcam 64715). Cocultures were then fixed and immunolabelled with antibodies against α-SMA (sigma A5228), Ki67 (ab15580) or active Caspase 3 (ab13847), revealed with Cy3- conjugated secondary antibodies. For each condition of each experiment, about 6-10 fields chosen randomly were recorded with a DMI 6000 Leica microscope connected to a Coolsnap camera at 20X magnification.

Molecular biology

TGFβ1 quantitation.

50000 BMDM were seeded in 96-well plates and polarized as described above. They were then washed twice with PBS and cultured in DMEM containing 0.1% BSA for 20 h. Sorted macrophages from fibrotic or regenerating muscle were directly collected in DMEM containing 0.1% BSA and cultured for 20 h. Conditioned medium was then harvested and centrifuged for 5 min at 2000 rpm. One part of the sample was used directly to determine the level of active TGFβ1 by ELISA (TGF beta-1 Human/Mouse Uncoated ELISA Kit, Invitrogen). To measure the level of total TGFβ1, the other part of the sample was subjected to heat denaturation followed by acidic treatment and neutralization according to the manufacturer's instructions.

qRT-PCR

Mouse BMDM and human fibroblasts (obtained from DMD or non-DMD patients, as described in (Desguerre et al., 2009) from Cochin Hospital Cell Bank, Paris, agreement no. DC-2009-944) were lyzed with TRIzol® reagent (Life Technologies) and total RNAs were separated from proteins and DNA with addition of chloroform. Sorted cells were collected in RLT+ Buffer (QIAGEN) and total RNAs were isolated using RNeasy Plus Micro kit (QIAGEN). RNAs were retro-transcribed into cDNA using Superscript II Reverse Transcriptase and qPCR was carried out in triplicate on a CFX Connect™ Real-Time PCR Detection System (Bio-Rad). Reaction mixtures had a final volume of 10 μl, consisting of 2 μl of cDNA, 5 μl of LightCycler® 480 SYBR Green I Master and 0.5 μM primers. After initial denaturation, amplification was performed at 95°C (10 s), 60°C (5 s) and 72°C (10 s) for 45 cycles. Calculation of relative expression was determined by the Bio-Rad CFX Manager™ software and fold change was normalized as Normalized Relative Quantity (or ΔΔCq) for each series, as $NRQ = \frac{2\Delta^{CqT-CqCal}}{2\Delta^{CqR-CqCal}}$ where T is the target sample, Cal the calibrator value (i.e., the mean of all sample Cqs of the serie) and R is the housekeeping gene Cyclophilin A for mouse or Ap3d1 for human. Log2-NRQ values were used to perform statistical analyses. Primer details are presented in Table S2.

QUANTIFICATION AND STATISTICAL ANALYSIS

Mouse histology

HE-stained muscle sections were recorded with a Nikon E800 microscope at 20X magnification connected to a QIMAGING camera. Necrotic myofibers were defined as pink pale patchy fibers, phagocyted myofibers were defined as pink pale fibers invaded by basophilic single cells (macrophages). Fluorescent immunolabelings were recorded with a DMI 6000 Leica microscope connected to a Coolsnap camera at 20X magnification. For confocal analysis, pictures were taken on a TCS SP5 X microscope (Leica Microsystems). For each condition of each experiment, at least 8-10 fields chosen randomly were counted. The number of labeled

macrophages was calculated using the cell tracker in ImageJ software and expressed as a percentage of total macrophages. Areas (PDGFR-α, Collagen 1) were calculated with ImageJ software. A macro was designed in ImageJ software to identify clusters containing small (< 200 μm^2) and large (> 200 μm^2) myofibers. The number of macrophages per fiber was counted in these areas defined using this macro (Figure S2). TGFβ1 mean fluorescence intensity (MFI) was measured using ImageJ. First, a mask was generated using either TGFβ1 or F4/80 labeling to select the areas of TGFβ1 or F4/80 expression. TGFβ1 MFI was then measured in both areas and the ratio of TGFβ1 MFI in F4/80 areas/ total TGFβ1 MFI was calculated.

Human histology

Analysis was performed for individual fascicles, which are easy to circumscribe. About 25-30 fascicles were analyzed. The number of cells was normalized for 100 myofibers.

Statistical Analyses

All experiments were performed using at least three different cultures or animals in independent experiments. The Student's t test, ANOVA or Spearman correlation test were used for statistical analyses. $p < 0.05$ was considered significant.